JANUARY 2019 M.Sc. in Electrical and Electronics Engineering MEHMET HALİL YABALAR

REPUBLIC OF TURKEY
UNIVERSITY OF GAZİANTEP
GRADUATE SCHOOL OF
NATURAL & APPLIED SCIENCES

DESIGN OF A MICROCONTROLLER BASED THREE PHASE INVERTER

M. Sc. THESIS
IN
ELECTRICAL AND ELECTRONICS ENGINEERING

BY
MEHMET HALİL YABALAR
JANUARY 2019

Design of a Microcontroller Based Three Phase Inverter

M.Sc. Thesis

in

Electrical and Electronics Engineering

University of Gaziantep

Supervisor

Prof. Dr. Ergun ERÇELEBİ

by

Mehmet Halil YABALAR

January 2019

REPUBLIC OF TURKEY
UNIVERSITY OF GAZİANTEP
GRADUATE SCHOOL OF NATURAL & APPLIED SCIENCES
ELECTRICAL-ELECTRONICS ENGINEERING

Name of the thesis: Design of a Microcontroller Based Three Phase Inverter

Name of the student: Mehmet Halil YABALAR

Exam date: 31.01.2019

Approval of the Graduate School of Natural and Applied Sciences

Prof. Dr. A. Necmeddin YAZICI
Director

I certify that this thesis satisfies all the requirements as a thesis for the degree of Master of Science.

Prof. Dr. Ergun ERÇELEBİ
Head of Department

This is to certify that we have read this thesis and that in our consensus opinion it is fully adequate, in scope and quality, as a thesis for the degree of Master of Science.

Prof. Dr. Ergun ERÇELEBİ
Supervisor

Examining Committee Members:	Signature
Prof. Dr. Ergun ERÇELEBİ	……………………
Prof. Dr. Celal KORAŞLI	……………………
Assoc. Prof. Dr. Ahmet Mete VURAL	……………………

I hereby declare that all information in this document has been obtained and presented in accordance with academic rules and ethical conduct. I also declare that, as required by these rules and conduct, I have fully cited and referenced all material and results that are not original to this work.

Mehmet Halil YABALAR

ABSTRACT

DESIGN OF A MICROCONTROLLER BASED THREE PHASE INVERTER

YABALAR, Mehmet Halil

M.Sc. in Electrical and Electronics Engineering

Supervisor: Prof. Dr. Ergun ERÇELEBİ

January 2019

54 pages

In this thesis, design and implementation of microcontroller based 3x200 W, 50 Hz three-phase inverter has been presented. The design of the three-phase sinusoidal pulse width modulation (SPWM) inverter model has been simulated by using electronic circuit design software named as Proteus. SPWM which is the most common method in inverter applications has been utilized in our design. SPWM method is characterized by fixed amplitude pulses with various duty cycles for each period. The widths of these pulses have been generated by microcontroller unit with sine Look-Up Table (LUT) in order to obtain inverter output voltage control and reduce its harmonics. SPWM as unipolar has been produced by ATmega 2560 microcontroller. The microcontroller-based three-phase inverter has 4 power MOSFET in each phase with H-Bridge topology after external shoot through circuit and MOSFET driver circuit. Unfiltered output of H-Bridge has been increased by step-up transformer. After transformer, the unfiltered output has been passed through Low-Pass Filter for having pure sine wave in 50 Hz. The transformers are connected in Y connection for stand-alone 3-Phase network. Finally, the hardware design for three-phase voltage switching SWPM inverter has been tested for different load conditions and calculated the efficiency for the best operational parameters. The test results showed that the design was successful.

Key Words: Microcontroller, SPWM, H-Bridge, Inverter

ÖZET

MİKRODENETLEYİCİ TABANLI ÜÇ FAZLI İNVERTÖR TASARIMI

YABALAR, Mehmet Halil

Yüksek Lisans Tezi, Elektrik ve Elektronik Mühendisliği

Tez Yöneticisi: Prof. Dr. Ergun ERÇELEBİ

Ocak 2019

54 sayfa

Bu tezde, mikro denetleyici tabanlı üç fazlı, 3x200 W, 50 Hz eviricinin tasarımı ve uygulaması sunulmuştur. Üç fazlı sinusoidal darbe genişlik modülasyonu (SDGM) eviricinin tasarımı Proteus olarak isimlendirilen elektronik devre tasarım yazılımı kullanılarak benzetimi yapılmıştır. Tasarımımızda evirici uygulamalarında en yaygın kullanılan yöntem olan SPWM kullanılmıştır. SDGM yöntemi, her döngü için çeşitli görev çevrimlerine sahip sabit genlikli darbeler ile karakterize edilmektedir. Bu darbe genişlikleri, eviricinin çıkış geriliminin kontrolünü sağlamak ve harmonikleri azaltmak için sinüs referans tablosu (SRT) ile mikro denetleyici kullanılarak üretilmiştir. Mikro denetleyici tabanlı üç fazlı evirici, her bir faz devresi için, harici kısa devre koruma devresi ve MOSFET sürücü devresinden sonra H-köprü topolojisine sahip 4 adet MOSFET'e sahiptir. H-Köprü'nün süzgeçlenmemiş çıkışı, yükseltici trafo ile arttırılmıştır. Trafodan sonra, süzgeçlenmiş çıkış saf sinüs dalgası için 50 Hz'de düşük geçişli süzgeç ile süzülmüştür. Transformatörler, şebekeden bağımsız 3-fazlı sistemlere bağlanmak için Y şeklinde bağlanmıştır. Son olarak, üç fazlı voltaj anahtarlamalı SDGM evirici için donanım tasarımı, farklı yük koşulları için test edilmiştir ve en iyi işletme parametreleri için verimliliği hesaplanmıştır. Test sonuçları tasarımın başarılı olduğunu göstermiştir.

Anahtar Kelimeler: Mikro denetleyici, Sinuoidal Darbe Genişlik Modülasyonu, H-Köprü, Evirici

"To my family"

ACKNOWLEDGEMETS

I would like to express my deepest gratitude to my supervisor Prof. Dr. Ergun ERÇELEBİ and co-supervisor Prof. Dr. Celal KORAŞLI for their guidance, advice, criticism, encouragements and insight throughout this study.

I would like to deeply and special thank to my wife for her patience, support and motivation during this project.

TABLE OF CONTENTS

Page

LIST OF TABLES

Page

LIST OF FIGURES

Page

LIST OF SYMBOLS / ABBREVIATIONS

UPS	Uninterruptible Power Supply
SPWM	Sinusoidal Pulse Width Modulation
PWM	Pulse Width Modulation
PCB	Printed Circuit Board
MI	Modulation Index
T	Period
Δt	Time Differences
HS	High Side
LS	Low Side
GND	Ground
DC	Direct Current
AC	Alternating Current
IC	Integrated Circuit
LUT	Look Up Table
HIN	High Input
LIN	Low Input
Vr	Reverence Signal Voltage
Vc	Carrier Signal Voltage
f_c	Carrier Frequency
R_{DS}	Drain-Source Resistor
V_{GS}	Gate-Source Voltage
V_{DC}	DC Battery Voltage
I_{DC}	DC Current
V_{L-N}	Line-to-Neutral Voltage
P_{IDLE}	Idle Power Consumption

CHAPTER 1

INTRODUCTION

1.1 Introduction

In last years, the demand in electrical energy has been increasing exponentially due to increase in population, economy growth and fast depletion of non-renewable energy sources i-e fossils therefore, renewable energy sources have been getting popularity worldwide and they have also no adverse effects on environment [1]. Therefore, electrical supply is the main problem in most countries; especially in Turkey. Turkey is the dependent country about energy supply. To reduce energy dependence, there are some alternative ways which can help in this purpose. However, among all of the methods, solar system may be an easy and effective one for energy supply. Solar energy popularity has been increasing. This solar energy is a renewable energy which is inefficiently exploited. The importance of solar energy is that it's free, clean and with very high potentials in the future. Therefore, inverters' importance is also increasing in power flow. The control of signals has become easily and stable thanks to developing microcontroller technology. In this way, it's very common to use microcontroller in power electronics.

Microcontroller based 3-phase inverter is a power electronic device that converts electrical energy from 24 V DC battery source to 220 V AC between line-neutral with 50Hz. There are two types of Pulse Width Modulation Inverters, voltage source and current source inverters depending on their energy storage components. Moreover, there are various common techniques in power electronics' literature for generating AC pure sine wave. However, sinusoidal pulse width modulation (SPWM) technique is applied for controlling the switching of mosfet in H-bridge to get pure sine wave AC output after step-up transformer and LC filter. SPWM produces pulses with fixed amplitude and variable duty cycles for each sample period. Normally, SPWM is generated by comparing triangle wave of carrier frequency and the sinusoidal signal of required frequency. All of these processes are executed by using a few ICs in constant configuration which provides static solution.

In this research, an alternative technique has been used for working a high computational powered 8-bit ATmega 2560 microcontroller for generating SPWM at requested frequency. It ensures dynamic solution to change the frequency of SPWM and to control algorithms without any modification in the hardware.

1.2 Problem Statement

On the market, many of 3-phase inverter devices are very expensive, that's why it is the aim of this project to design a DC/AC 3-phase inverter suitable for producing a pure sine wave using cheap but quality equipment. In this research, 3-phase inverter circuit has been designed that can supply any load up to 3x200 W.

1.3 Objectives

The main objective of this project is that design, simulation and hardware implementation of 3-phase inverter which has 3x200 W rated power that converts 24 V DC to 220V AC for line-neutral potential. The system's main characteristics are;

- Generation of pure sine wave signal
- Minimization of circuit complexity by microcontroller to generate control signal.

1.4 General Outline of the Thesis

This project is organized in six chapters.
Chapter 1: This chapter gives a general introduction, project objective and what need for power inverter.

Chapter 2: This chapter gives the theory and background information concerning the power inverter. The principles of operation of three phase inverter are outlined here. The performance parameters are also described.

Chapter 3: This chapter describes the system design. Operation of inverter and how it is used to realize a power inverter is described in this chapter. A three-phase simulation of an inverter is described and modelled.

Chapter 4: This chapter includes a complete design and implementation of study with Arduino MEGA 2560 microcontroller.

Chapter 5: This chapter includes results and analysis of 3-Phase inverter with practical results.

Chapter 6: This chapter includes conclusions and recommendation for the future work on this project.

CHAPTER 2

LITERATURE REVIEW

There are many applications in which it is necessary to control the output voltage of the inverter. Two such application are a stabilized AC or DC voltage source from a battery whose voltage varies during discharge, and an AC motor control system, in which a constant voltage-to-frequency ratio has to be maintained to avoid saturation of the motor. In both cases, control of inverter output voltage is necessary [2].

The common methods of output control are:

• Controlling DC input voltage

• Controlling AC output voltage

• Pulse width modulation

If inverter is supplied from an AC source through a rectifier, the input to the inverter can be regulated by means of an induction regulator, variac or a controlled rectifier. If the supply is DC, it can be regulated by shunt or series regulator or chopper using time-ratio control method. The pulse width modulation can be applied for both types of inputs. For this purpose, PWM is explained in the next section.

2.1 Pulse Width Modulation (PWM)

PWM is the technique of obtaining the analogue electrical value or signal to be produced at the output by controlling the width of the pulses to be produced [3].

There are some types of PWM methods. Therefore, it is possible to obtain different outputs and the selection of DC/AC converter depends on price, efficiency and noise or harmonic ratio.

The most important parameter is duty cycle which is the ratio of time circuit is on position compared to the time the circuit is off position. It is expressed in Equation 2.2.

2.1.1 Basic PWM Techniques

There are three basic PWM techniques.

i) Single Pulse Width Modulation

ii) Multiple Pulse Width Modulation

iii) Sinusoidal Pulse Width Modulation

These techniques are able to produce modulated output voltages used applicable in almost all inverter applications.

2.1.2 Single Pulse Width Modulation

In this modulation method there is only one output pulse per half cycle. The output has been changed by varying the width of the pulses. The gating signals have been generated by comparing a rectangular reference with a triangular signal. The frequency of the two signals is almost equal [4].

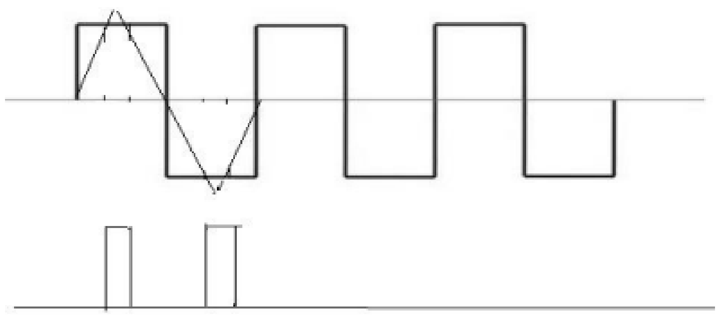

Figure 2.1 Single pulse width modulation

The rms AC output voltage can be calculated in Equation 2.1:

$$V_O = V_S\sqrt{\frac{2t_{on}}{T}} = V_S\sqrt{2\delta} \qquad (2.1)$$

where,

$$\text{Duty Cycle} = \delta = \frac{t_{on}}{T} \qquad (2.2)$$

$$\text{Modulation Index (MI)} = \frac{V_r}{V_c} \qquad (2.3)$$

By varying the control signal amplitude V_r (Reference) from 0 to V_c (Carrier) the pulse width ton can be changed from 0 second to T/2 second and the rms output voltage V_o from 0 to V_s.

2.1.3 Multiple Pulse Width Modulation

In this technique, the harmonic content can be decreased by using several pulses in each half cycle of output voltage. The gate signals have been produced by comparing reference signal with triangular carrier signal. The frequency of the reference signal sets the output frequency (f_o) and carrier frequency (f_c) determines the number of pulses (p) per half cycle; [5]

$$p = \frac{f_C}{2f_O} \tag{2.4}$$

The rms AC output voltage can be calculated in equation 2.5:

$$V_O = V_S\sqrt{\frac{p\delta}{\pi}} \tag{2.5}$$

where,

$$\text{Duty Cycle} = \delta = \frac{t_{on}}{T} \tag{2.6}$$

The variation of modulation index (MI) from 0 to 1 varies the pulse from 0 to π/p and the output voltage from 0 to V_m.

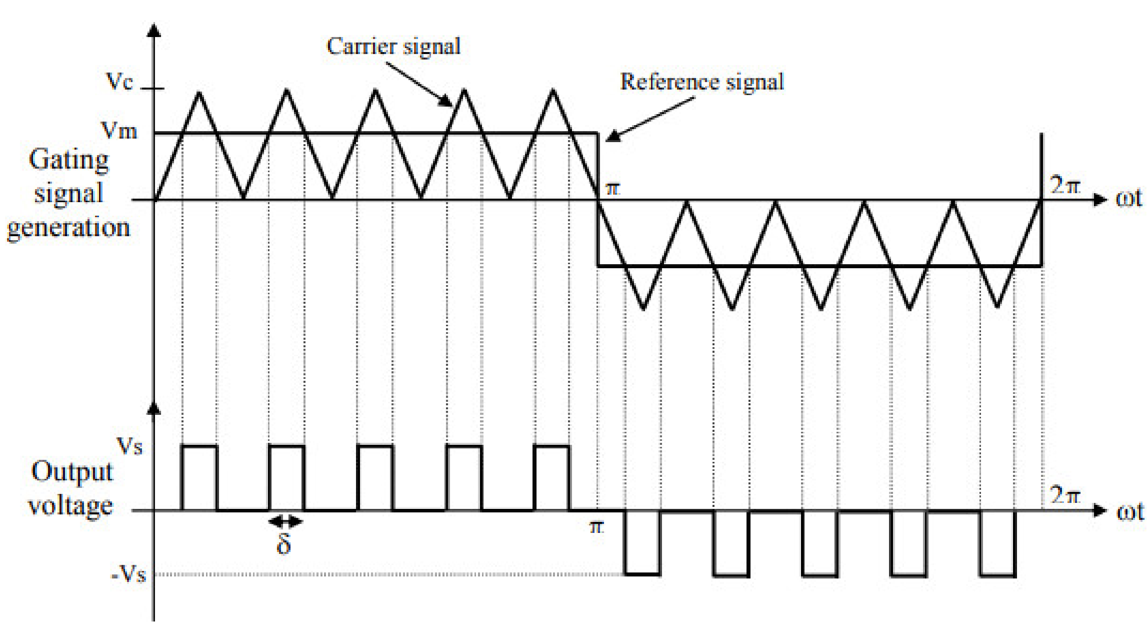

Figure 2.2 Multiple pulse width modulation [5]

2.1.4 Sinusoidal Pulse Width Modulation

The generation of a sinusoidal PWM signal with this technique is shown in Figure 2.3. The gating signal can be produced by comparing a sinusoidal reference signal with a triangular carrier wave and the width of each pulse varied proportionally to the amplitude of a sine wave evaluated at the center of the same pulse [6].

The rms AC output voltage is:

$$V_O = V_S\sqrt{\frac{p\delta}{\pi}} \rightarrow V_S\sqrt{\sum_{n=1}^{2\pi}\frac{\delta_n}{\pi}} \quad (2.7)$$

where,

p=number of pulses

δ= pulse width

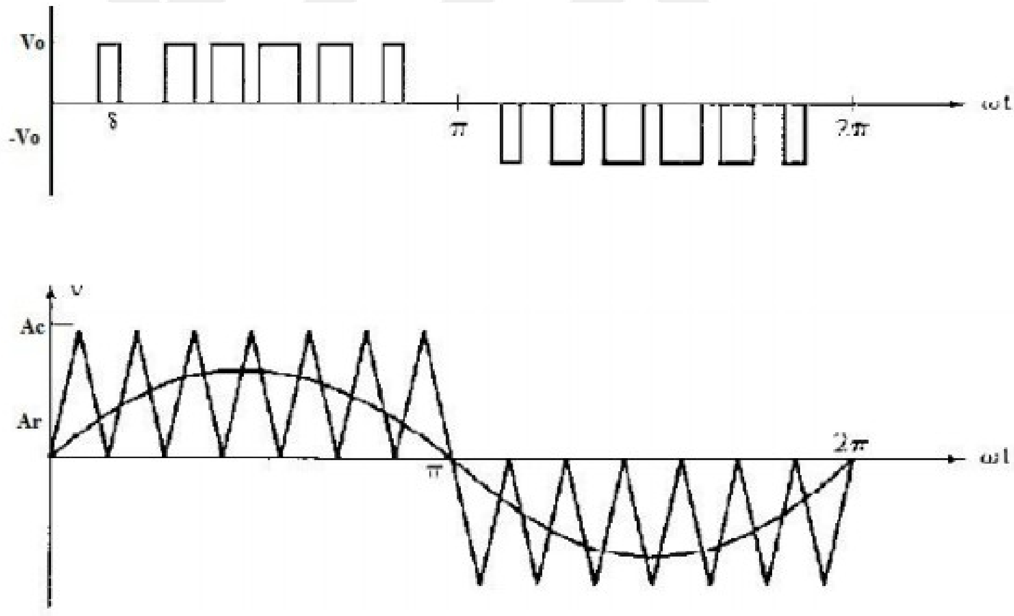

Figure 2.3 Sinusoidal Pulse Width Modulation [4]

2.2 Inverter Types

DC/AC converters are known as inverters. The function of an inverter is that changing a DC input voltage to a symmetric AC output voltage of required amplitude and frequency. There are three types of inverters: [7]

(i) Square wave inverter

(ii) Modified square wave inverter

(iii) Pure sine wave inverter

2.2.1 Square Wave Inverter

Square wave inverter is the simplest type of inverter. The output of inverter is look like alternating square wave. It has very large undesired harmonics. Square wave inverter is not efficient. It may cause serious damage to some of the electronic equipment. It can be only preferable due to low cost. Otherwise, it is not as good as other sine wave inverter or modified sine wave inverter. Therefore, it has limited applications in household appliances.

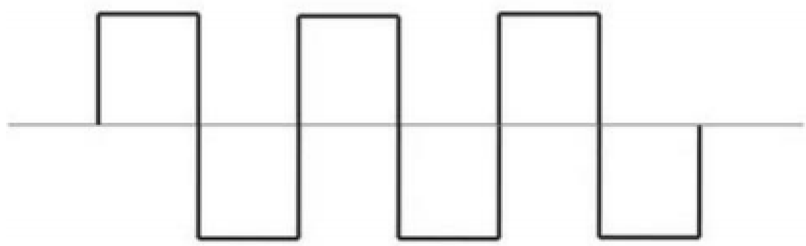

Figure 2.4 Square wave ınverter

2.2.2 Modified Square Wave Inverter

A modified square (or sine) wave is similar to a square wave but instead has a “stepping” look to it that relates more in shape to a sine wave. It is clear that in Figure 2.5, how a modified square wave tries to emulate the sine wave itself. The waveform is easy to produce, as it is just the product of switching between 3 values at desired frequencies. The modified square wave inverter provides a cheap and easy solution to powering devices which work with AC power. It does have some drawbacks as not all devices work properly on a modified square wave, products. For example, computers and medical equipment are not resistant to the distortion due to the harmonics [8].

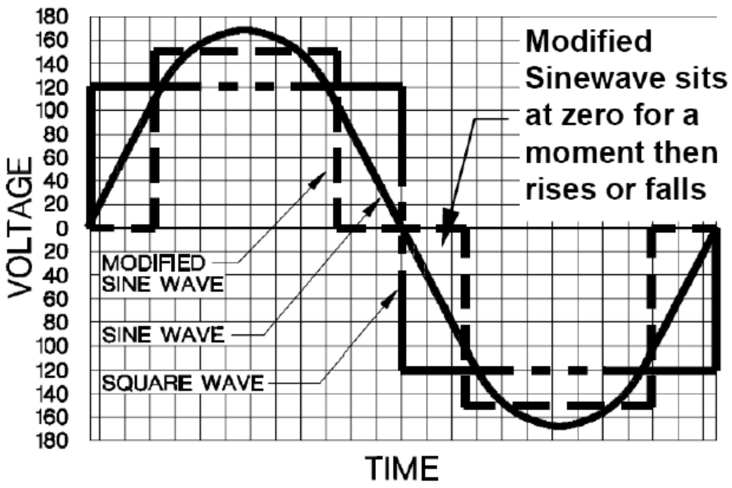

Figure 2.5 Square, modified and pure sine wave [8]

2.2.3 Pure Sine Wave Inverter

Pure sine wave inverter provides output voltage waveform which is very close to the voltage waveform that is received from the Grid. The sine wave has little harmonic contents resulting in a very "clean" supply and makes it ideal for running electronic systems such as computers, digital fix racks and other sensitive equipment without causing problems or noise. Other equipments like mains battery chargers also run better on pure sine wave converter [3].

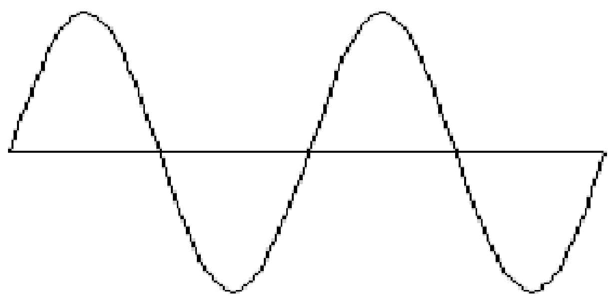

Figure 2.6 Pure sine wave inverter

Benefits of using pure sine wave inverter are;

- Most of the electronic equipment's have been designed for the pure sine wave.
- Some appliances like variable motor, refrigerator, microwave will not be able to provide rated output without sine wave supply.
- Electronic clocks are designed for the sine wave.
- Harmonic content of this type of inverter is less [4].

2.3 H-Bridge Configuration

H-Bridge type or full-bridge converter is a switching configuration with four switches in a combination that resembles H symbol. By controlling different mosfets in the bridge, positive, negative, or zero-potential voltage can be measured across a load [8].

D1, D2, D3 and D4 provide a bypass path for the current across the switching semiconductor devices. This is done by connecting diodes across the semiconductor switches or semiconductors having body diode. The diodes are referred to as feedback or free-wheeling diodes. They operate as rectifiers permitting reverse energy to flow from the load to the source. (see Figure 2.7.)

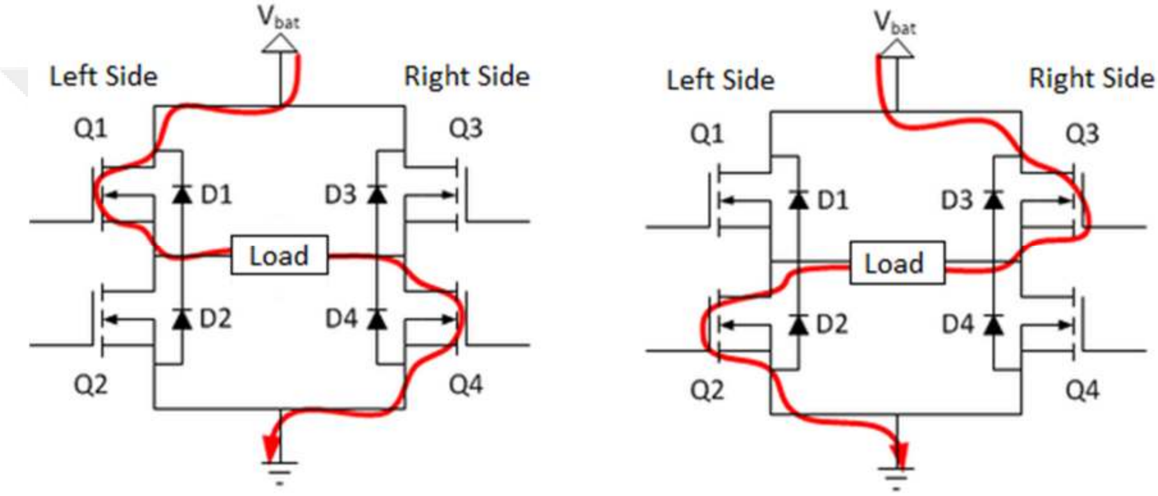

Figure 2.7 H-bridge power flow

H bridge circuit has four mosfet as swithcing components (Q1, Q2, Q3 and Q4). There are four conditions with these switching mosfets. These conditions are listed in Table 2.1. All the other conditions are declined; because, other conditions are called as shoot through circuit which means short circuit between V_{BAT} to GND, it can damage to the mosfets, drivers or other components.

Table 2.1 H-bridge truth table

Q1	Q2	Q3	Q4	V_{output}
ON (Closed)	OFF (Opened)	OFF (Opened)	ON (Closed)	$+V_{BAT}$
OFF (Opened)	ON (Closed)	ON (Closed)	OFF (Opened)	$-V_{BAT}$
ON (Closed)	OFF (Opened)	ON (Closed)	OFF (Opened)	Zero
OFF (Opened)	ON (Closed)	OFF (Opened)	ON (Closed)	Zero

2.4 Shoot-Through Circuit

An important short-circuit condition called shoot-through occurs when both the high side and low side power mosfets are closed at the same time. Shoot-through can happen even if it never intends to have both mosfets on simultaneously. For example, when the high side mosfet is turned on and the low side mosfet is turned off, logic propagation delay and the time required for charging or discharging the mosfets' gate capacitances may cause a short time when high side mosfet is half on and the low side mosfet is half off. The current flows from V_{CC} to GND through both mosfets, it is called shoot-through [9].

As shown in Figure 2.8, current flows from V_{bat} to GND via A side Q1 and Q2 mosfets having very small drain source resistance. This currents may rush in transient shoot-through time. It may cause PCB ways or other components damage.

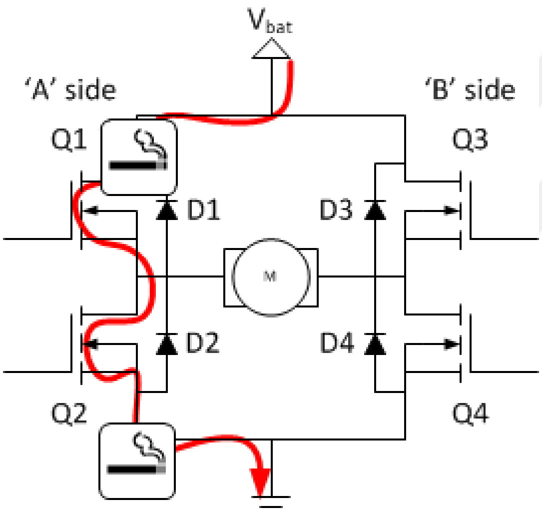

Figure 2.8 Shoot-through circuit

Figure 2.9 shows that PWM0 waits just a little time after PWM1 falling edge, because; Q2 mosfet's gate miller capacitance should be discharged. Also, PWM1 waits just a little time after PWM0 falling edge with same reason [10].

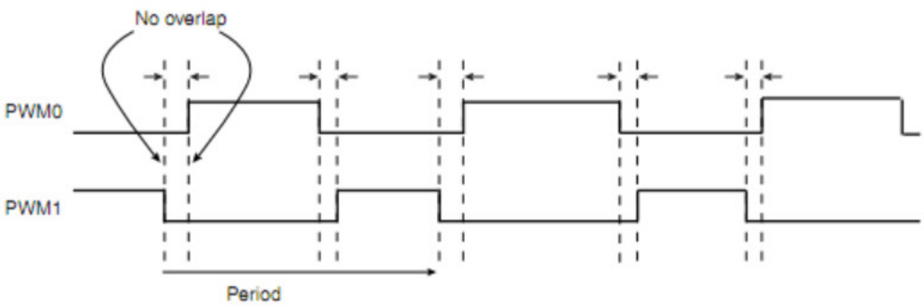

Figure 2.9 Dead time for turn-on and turn-off [10]

2.5 Snubber Circuits

Snubber capacitors may be applied to protect fast switching semiconductors from voltage transients while turning-on and turning-off. Snubber circuits or only capacitors can be placed across the switching devices for protection and high performance. Snubbers have some features which are:

- Reducing or elimination voltage or current spikes
- Limiting dI/dt or dV/dt
- Shaping the load line to keep it within the safe operating area (SOA)
- Transfering power dissipation from the switch to a resistor or a useful load
- Reducing total losses due to switching
- Reducing EMI by damping voltage and current ringing

Figure 2.10 Snubber Capacitor

CHAPTER 3

METHODOLOGY

3.1 Modeling

In this chapter, 3-Phase SPWM microcontroller based pure sine wave inverter has been implemeted in Proteus Software. As shown in Figure 3.1, SPWM signals generated by ATmega 2560 drive Mosfet Driver ICs. H-Bridge Topology has been controlled by driver signals and applied 24 V DC battery source. Subsequently, step-up transformer increases the voltage to unfiltered 311 V_{peak}. LC filter has been canceled the oscillator frequency and other undesired harmonics. Finally, 220 V AC line-to-neutral with 50 Hz pure sine wave has been generated. Table 3.1 shows that the characteristics of present three-phase inverter.

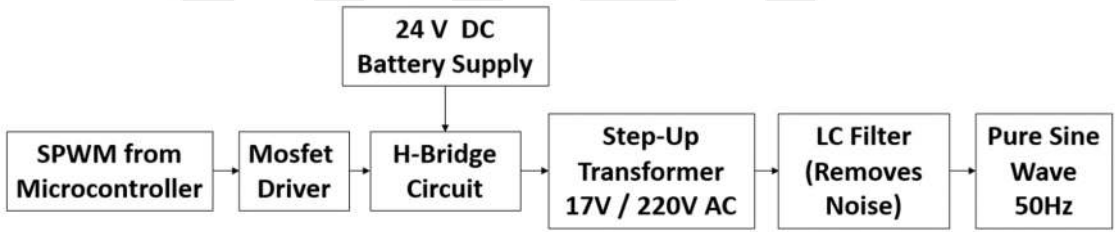

Figure 3.1 DC to AC conversion flow chart diagram

Table 3.1 Three-phase inverter characteristics

Number of Phase	3-Phase
Phase-Phase Voltage	380 V
Maximum Power	3x200W = 600W
Frequency	50 Hz
Input Battery Voltage	24 V DC
SPWM Frequency	16 kHz

3.2 Sine Look-Up Table

A sine wave is an analog signal and it's necessary to make digitally for microcontroller processing. Sine look up table is representation of analog sine wave with using square waves. SmartSine is a special calculator which generates a single or more cycles sine wave LUT (Look-up table). In this way, this application is functional operation in order to synthesize sine waves digitally.

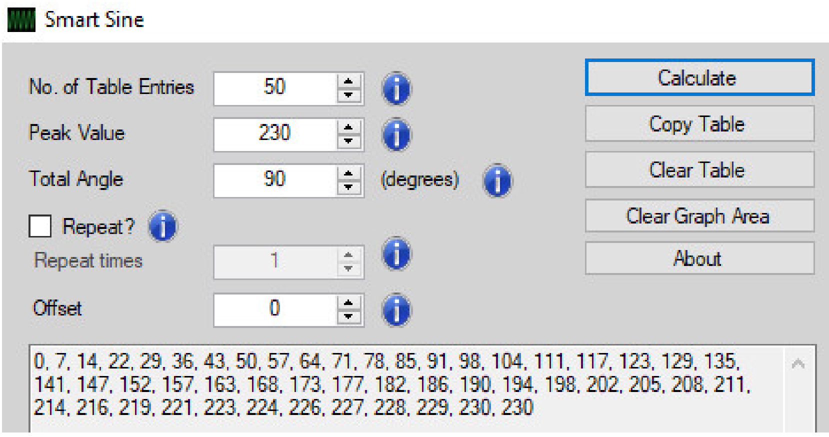

Figure 3.2 SmartSine application parameters

There is a quarter of full period sine wave with 50 samples in Figure 3.2. All of these 50 values represent a duty cycle for each index. The data of 50 samples for one quarter of a sine wave generated by SmartSine calculator is plotted in Figure 3.3.

Normally, its peak value is 255 because of 8 bits microcontroller. However, it is chosen 230 to avoid damage to Mosfet due to enough discharging time of gate miller capacitance. The PWM's timing resistor and capacitor should be selected for the maximum "ON" time and minimum "DEAD" time of the PWM output [11]. Therefore, the maximum duty cycle should be %90 because of existing the external shoot through circuit. There is some waiting interval time for protection, that's why it cannot be used with 100% duty cycle.

$$\%90\ Duty\ Cycle = \%90 * 255 = 230 \tag{3.1}$$

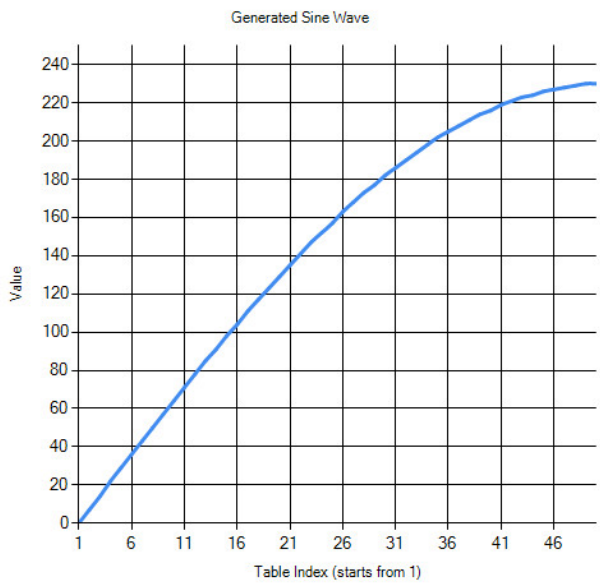

Figure 3.3 Sine look-up table (LUT) for 90°

3.3 Generating Control Signals

There are 3 different SPWM and 3 different 50 Hz PWM generated by Arduino Mega 2560 for 3-Phase inverter. According to the 3-Phase Power System Theory, the first phase has been taken as reference which is 0° phase aligned. The second phase has 120° phase shifted and the third phase has 240° phase shifted. This phase difference has been made by Arduino with different beginning time.

3.4 External Shoot-Through Protection Circuits

If integretad circuit mosfet driver does not have any shoot-through protection circuit via turn-on and turn-off delay, it must be designed external protection circuit as shown in Figure 3.4 [10].

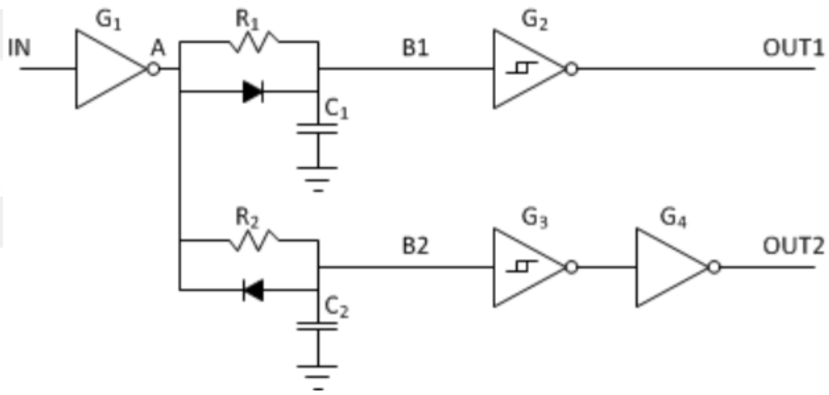

Figure 3.4 Shoot-through protection circuits [10]

It's clear that how this circuit reproduces the same non-overlapping outputs that can be seen in Figure 3.5. The delay of the falling edge of OUT1 can be calculated as:

$$t_{delay,OUT1} = -R_1C_1In(\frac{V_{t1}}{V_{oh}}) \tag{3.2}$$

Where V_{oh} is the high-level output voltage of the input gate, and V_{tl} is the low-level trigger voltage of the Schmitt-trigger. Similarly, the delay of the rising edge of OUT2 is; [10]

$$t_{delay,OUT2} = -R_2C_2In(1-\frac{V_{th}}{V_{oh}}) \tag{3.3}$$

Where V_{th} is the high-level trigger voltage of the Schmitt-trigger.

With many Schmitt-trigger circuits having their lower and higher threshold voltages set at 1/3 and 2/3 way between 0 and V_{oh}, both time delays end up roughly with time constants R_1C_1 and R_2C_2 respectively. [10]

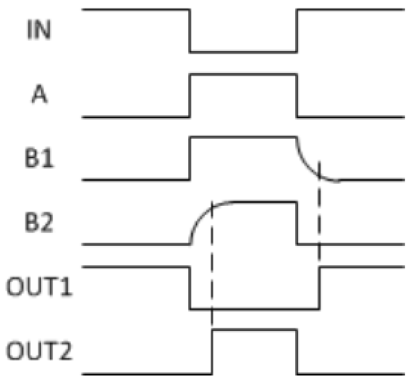

Figure 3.5 Shoot-through protection signals

As shown in Figure 3.6, 4093 NAND Schmitt Trigger has been modified the signal as wave shaper. It has been used for external shoot-through protection signals.

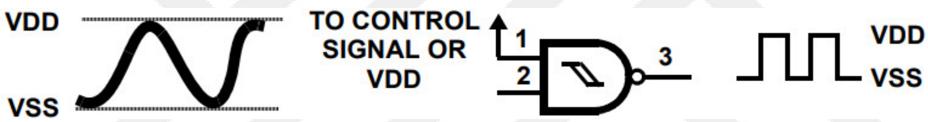

Figure 3.6 Wave shaper for 4093 NAND schmitt triggers

The left side of H-bridge circuit is given in Figure 3.7.

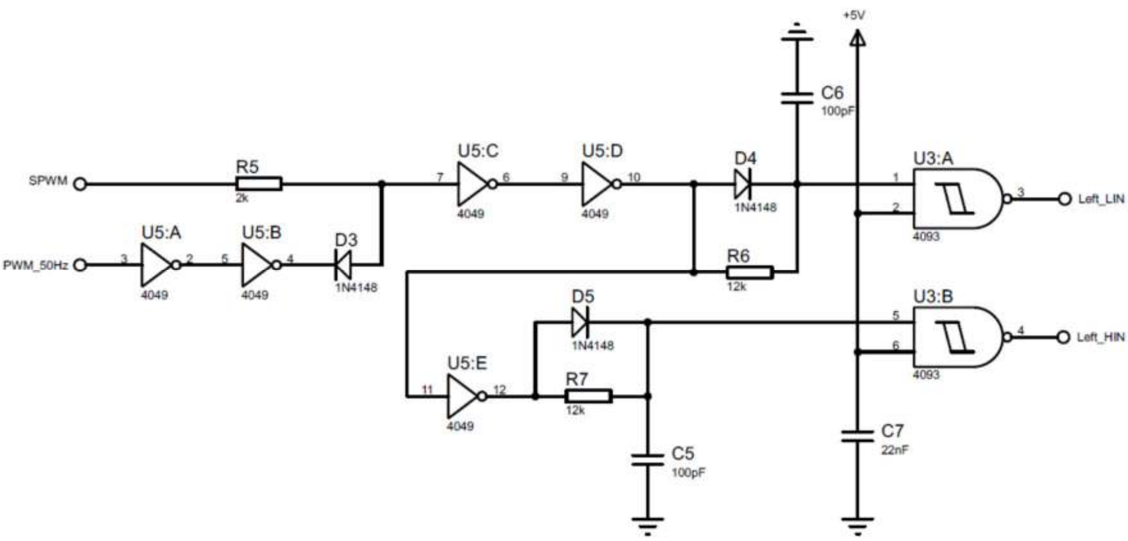

Figure 3.7 Control signals for left-side of H-bridge circuit

The delay time of this part (OUT1) is expressed using the result of Equation 3.2 as:

$$t_{delay,OUT1} = -12k \times 100p \times \mathrm{In}\left(\frac{3.5\ V}{4.95\ V}\right) = 0.41\ \mu s \qquad (3.4)$$

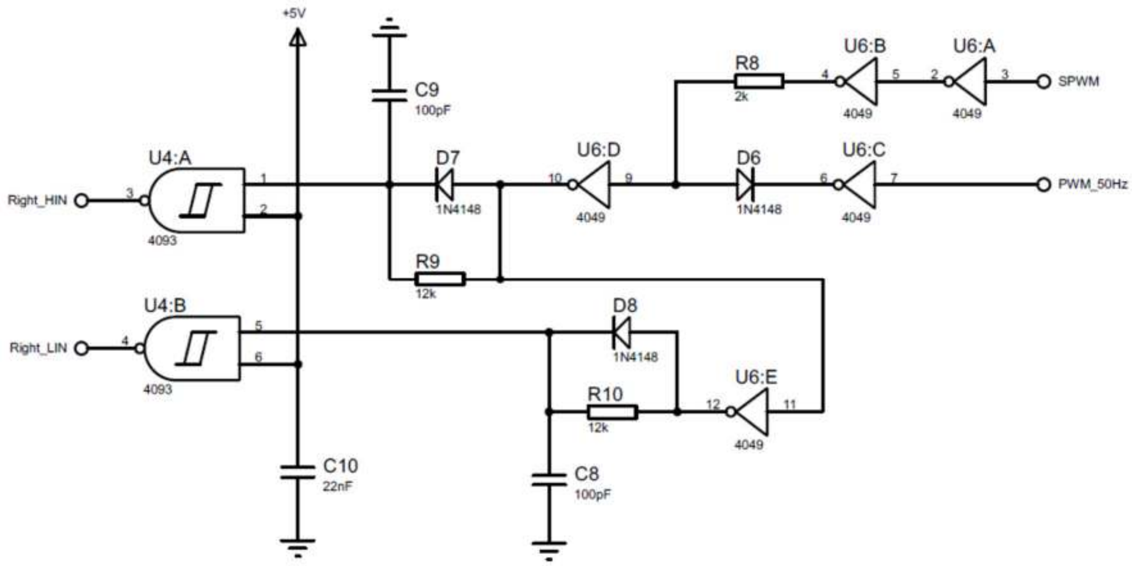

Figure 3.8 Control signals for right-side of H-bridge circuit

Similarly, the Right-Side of H-Bridge circuit shown in Figure 3.8 produces the delay time expressed in Equation 3.3 which is resulted by making use of Equation 3.5.

$$t_{delay,OUT2} = -12k \times 100p \times \text{In}\left(1 - \frac{1.9\ V}{4.95\ V}\right) = 0.58\ \mu s \qquad (3.5)$$

3.5 Mosfet Driver

The output of the microcontroller can not drive the gates for the CMOS logic inverter because the threshold voltage for the mosfets are 4.5 V. [12] Power Mosfets have large stray capacitance between the gate and source. The effect of this is that the gate voltage must first charge the capacitance before the gate is turned on. For efficient switching instants of the mosfets, the gate drive voltage need to be in the range of 10-20 V depending on the device rating. A simple integrated circuit IR2112 mosfet driver has been used for this design as shown in Figure 3.9. [13]

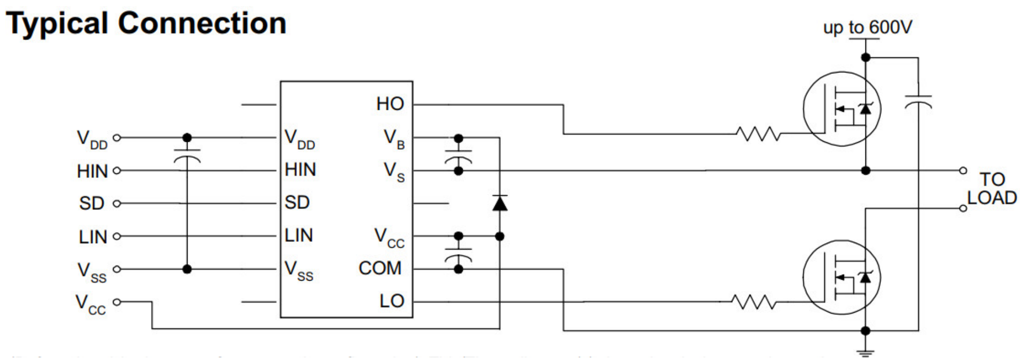

Figure 3.9 Typical connection for IR2112 mosfet driver

3.5.1 Basics of Gate Drive Requirement

Gate Driver is a power amplifier that accepts a low-power input from a controller IC and produces the appropriate high-current gate drive for a power MOSFET. The gate driver must source and sink current to establish required V_{GS}. A gate driver is used when a pulse width- modulation (PWM) controller cannot provide the output current required to drive the gate capacitance of the MOSFET. Gate drivers may be implemented as dedicated ICs, discrete transistors, or transformers. They can also be integrated within a controller IC. Partitioning the gate-drive function off the PWM controller allows the controller to run cooler and be more stable by eliminating the high peak currents and heat dissipation needed to drive a power MOSFET at very high frequencies. [14]

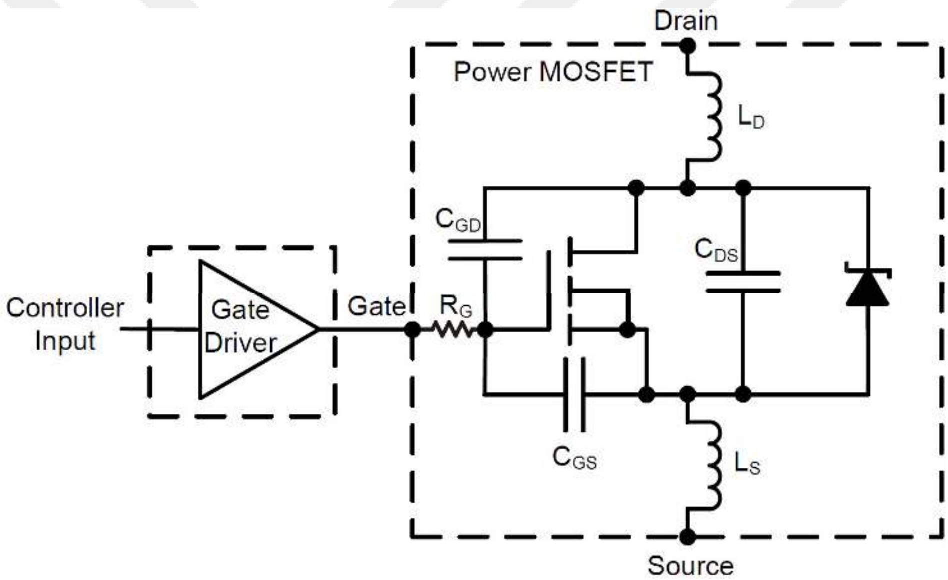

Figure 3.10 Simplified model of non-inverting gate driver IC and mosfet

A real mosfet is a voltage-controlled switch having the following properties:

• Inherent parasitic capacitors.

• R_{DS} (ON) is not negligible.

This leads to the requirement of Gate driver which must source and sink current to establish required threshold voltage from Gate to Source V_{GS} [14].

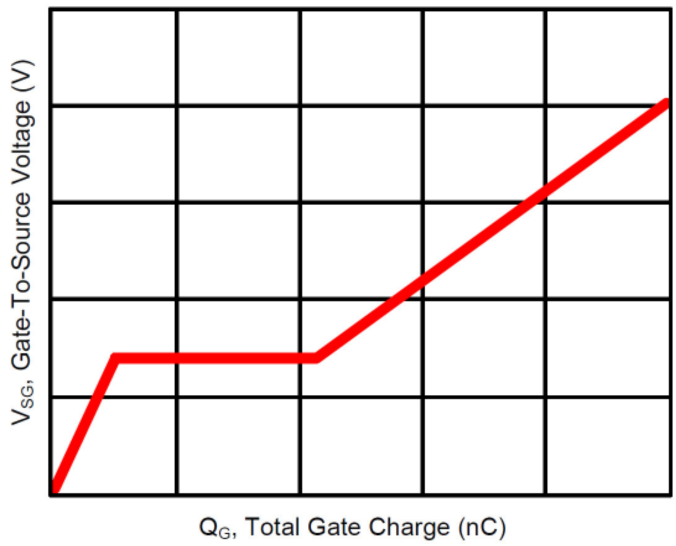

Figure 3.11 Power mosfet gate drive characteristics

Figure 3.11 shows total gate charge as a function of the gate-drive voltage of a power mosfet. Total gate charge (QG) is how much can be applied to the mosfet gate to reach fully turn-on. It is generally specified in nanocoulombs (nC). It is required in Table 3.2 for calculation of bootstrap capacitor [14].

3.5.2 Bootstrap circuit Principle for High Side Gate Drive

The Bootstrap supply method is a simple, cost-effective way to power the upper mosfet's gate and provide bias supply to the floating the gate driver. Only two components (a Bootstrap diode and capacitance) per bridge phase are required to implement the Bootstrap supply [14].

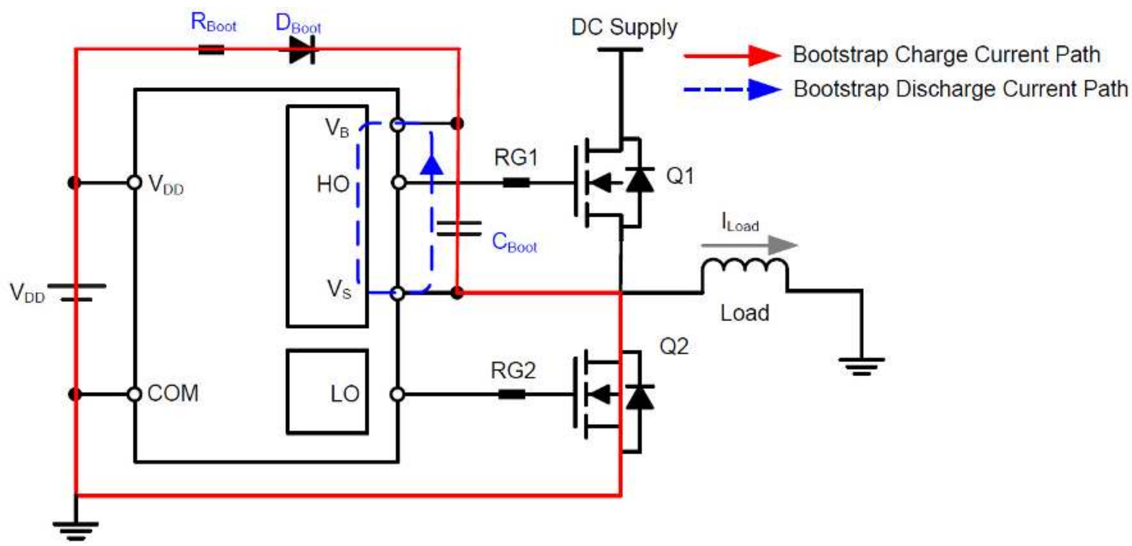

Figure 3.12 Bootstrap supply circuit

As shown in Figure 3.12, the Bootstrap Capacitor is charged to ground through the low side mosfet. When the Low side mosfet is turned off, the bottom of the capacitor flies up and it creates a voltage greater than V_{DD}. This voltage is applied to the high side of gate driver [15].

3.5.3 Bootstrap Capacitor

As shown in Figure 3.12, the bootstrap diode and capacitor are the only external components strictly required for operation in a standard PWM application. Local decoupling capacitors on the V_{CC} (and digital) supply are useful in practice to compensate for the inductance of the supply lines [12].

The minimum bootstrap capacitor value has been calculated from the following equation [16];

$$C \geq \frac{2\left[2Q_g + \frac{I_{qbs(max)}}{f} + Q_{Is} + \frac{I_{Cbs(leak)}}{f}\right]}{V_{cc} - V_f - V_{LS} - V_{Min}} \tag{3.6}$$

The parameters of variables are given in Table 3.2.

Table 3.2 Bootstrap capacitor calculation parameters [16]

Symbol	Name	Value
Q_g	Gate charge of High-Side FET	130 nC
f	Frequency of operation	16 kHz
$I_{Cbs(leak)}$	Bootstrap capacitor leakage current	250 µA
$I_{qbs(max)}$	Maximum V_{BS} quiescent current	60 µA
V_{cc}	Logic section voltage source	15 V
V_f	Forward voltage drop across the bootstrap diode (SB1100 Schottky Diode)	0.8 V
V_{LS}	Voltage drop across the low-side FET or Load	1.3 V
V_{Min}	Minimum voltage between V_B and V_S	10 V
Qls	Level shift charge required per cycle (typically 5nC for 500 V/600 V MGDs and 20nC for 1200 V MGDs)	5 nC

All the values given in Table 3.2. are taken substituted into Equation 3.7 from the driver for IR2112 IC datasheet and IRF1010e MOSFET datasheet. Using these parameters minimum bootstrap capacitance has been calculated as;

$$C \geq \frac{2\left[2 * 130 * 10^{-9} + \frac{60 * 10^{-6}}{16000} + 5 * 10^{-9} + \frac{250 * 10^{-6}}{16000}\right]}{15 - 0.8 - 1.3 - 10} \quad (3.7)$$

$$C \geq 0.196\ \mu F$$

The bootstrap capacitor value determined from the Equation 3.7 is the extremely minimum value. However, according to the nature of bootstrap circuit operation, a low value capacitor may lead to overcharge which may cause damage the IC. Thus, to reduce the risk of overcharging and ripple on the drain-source voltage, the capacitor tolerated value should be calculated by as a multiple of 0.196 μF value which is 15 in order to get optimum capacitor value which is nearly 2.2 μF [12].

3.6 H-Bridge Circuit

An open circuit of the H-Bridge with mosfet IRF1010e and IR2112 mosfet drivers are shown in Figure 3.13.

D9, D10, D11 and D12 schottky diodes discharge the gate capacitances (miller capacitance) of MOSFET quickly, bypassing the gate resistors, decreasing the turn off time. R1, R2, R3 and R4 are the gate current-limiting resistors.

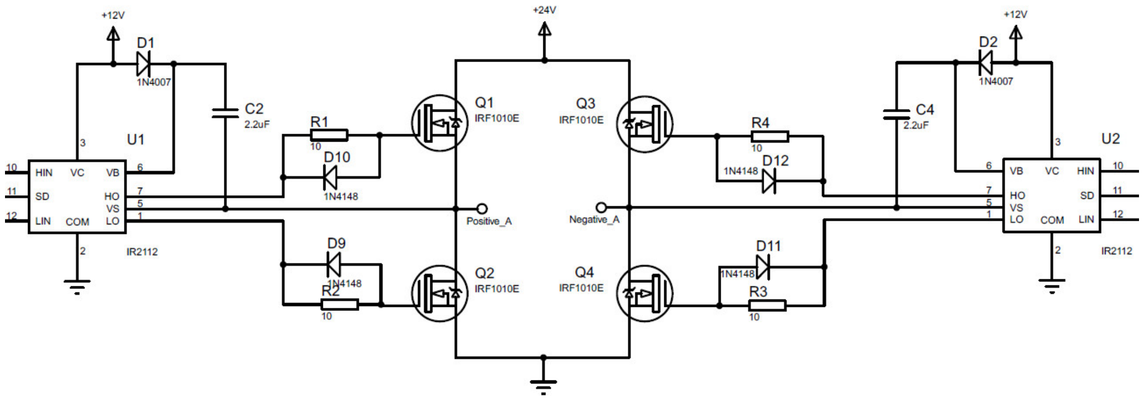

Figure 3.13 H-bridge circuit with mosfet drivers

H-Bridge shown in Figure 3.13 is designed using four Mosfet for switching. When switch Q1 and Q4 are closed and switches Q2 and Q3 are opened, a positive alternans will be appeared across the load between output of left side and right side. By closing Q2 and Q3 mosfets and opening Q1 and Q4 mosfets a reverse voltage will be applied across the load.

Driving four mosfets for switching in a H-Bridge topology allows +24 V, -24 V, or 0 V across the primary side of the transformer. The left side and right side of the H-Bridge has been driven by different control signals which are Left-LO, Left-HO, Right-LO, Right-HO on Mosfet Driver. The 50 Hz square wave has been controled the polarity of the output pure sine wave, while the Sinusoidal-PWM signal has been controled the amplitude of output. The switching instrument is IRF1010E Mosfet in the design, rated for 60 V at 84 A with a R_{DS} of 12 mΩ is given in datasheet.

CHAPTER 4

IMPLEMENTATION

4.1 Simulation and Actual Results

4.1.1 SPWM & PWM Signals

Figure 4.1 shows that left side of H-bridge before mosfet driver.

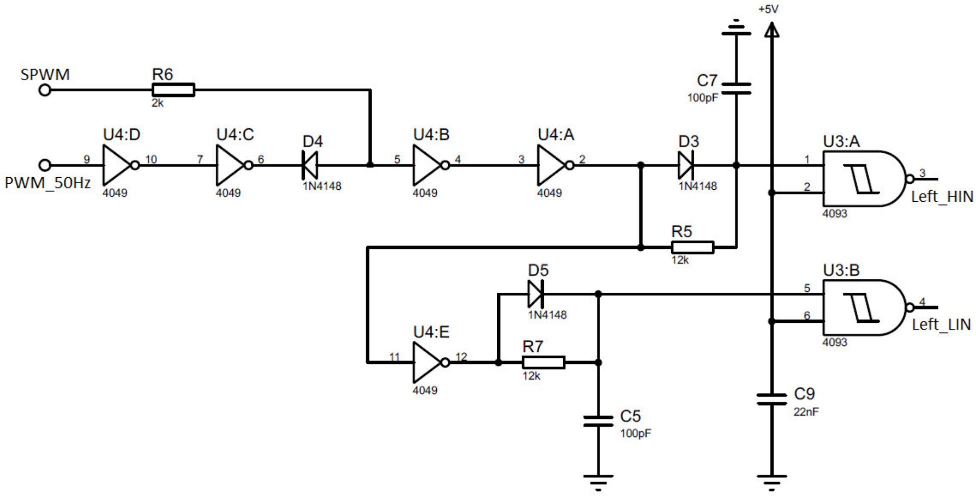

Figure 4.1 Left side of H-bridge before mosfet driver

Figure 4.2 displays simulations results of Left_HIN and Left_LIN are generated by multiplication of SPWM and PWM_50Hz. Left_HIN is always complement of Left_LIN.

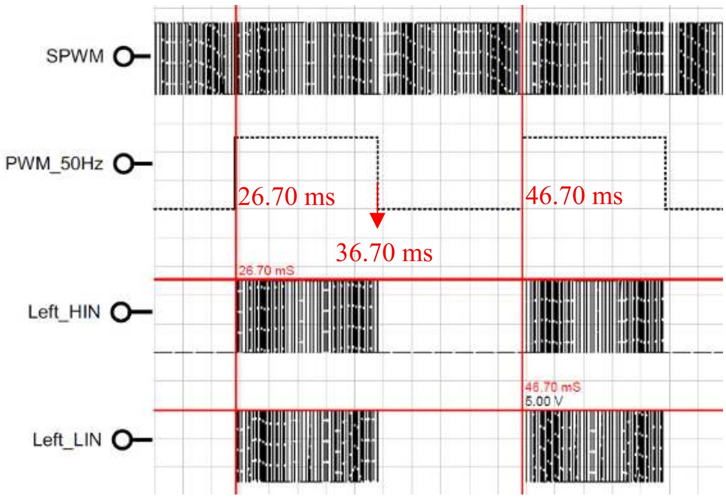

Figure 4.2 Simulation results of multiplication between SPWM and PWM_50Hz

As shown in Figure 4.3, actual oscilloscope results of SPWM and PWM_50 Hz of reference phase. It is also verified by simulation results in Figure 4.2.

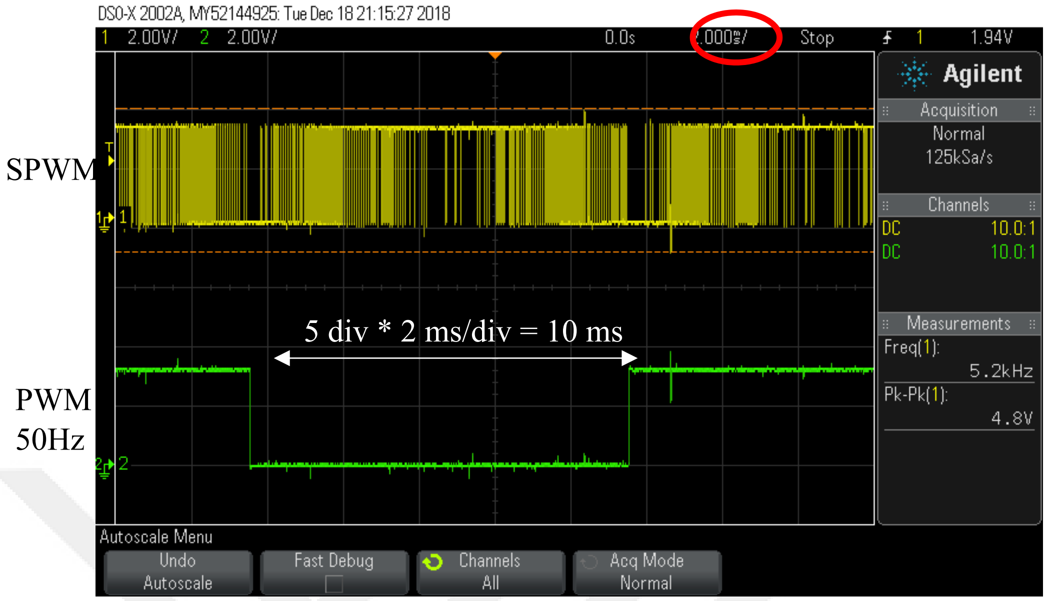

Figure 4.3 Actual scope Results of SPWM and PWM 50Hz

There are some sample pulses of SPWM in Figure 4.4. The first rising edge time is -3.77 ms and the second rising edge time -3.71 ms. The time difference is 0.06 ms between these two rising edges. The SPWM frequency is expressed in Equation 4.1.

$$f_{SPWM} = \frac{1}{\Delta T} = \frac{1}{0.06 \text{ ms}} \approx 16 \text{ kHz} \tag{4.1}$$

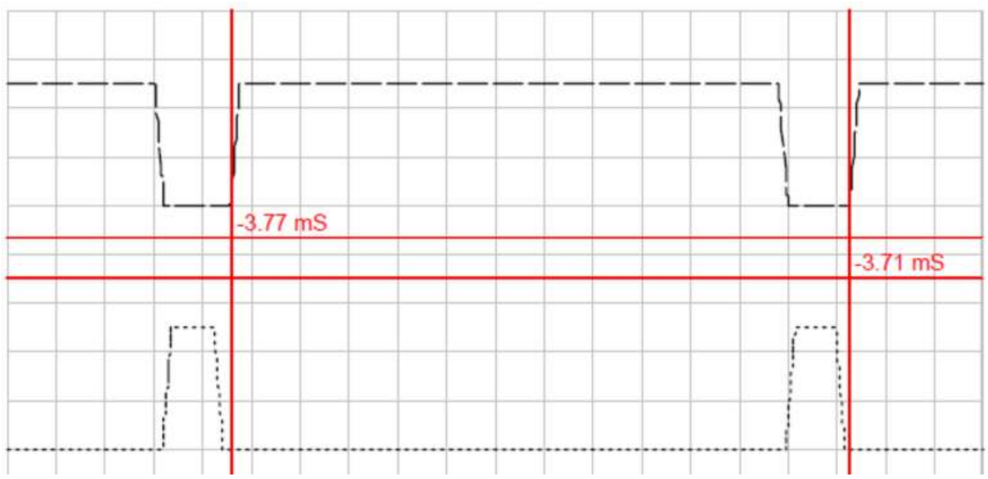

Figure 4.4 SPWM rising edges

4.1.2 PWM Phase Differences

As shown in Figure 4.5, yellow colored signal has been rised at the time 9.80 ms, blue colored signal has been rised at the time 16.50 ms, purple colored signal has been rised at the time 23.10 ms. It is clear that the time difference between the first and second signal is about 6.7 ms. Moreover, the time difference between the second and third signal is about 6.6 ms (23.10 ms – 16.50 ms).

$$\Delta t_1 = 16.50 \text{ ms} - 9.80 \text{ ms} = 6.7 \text{ ms} \tag{4.2}$$

$$\Delta t_2 = 23.10 \text{ ms} - 16.50 \text{ ms} = 6.6 \text{ ms} \tag{4.3}$$

Since the period of 50 Hz sine wave is 20 ms, Phase_A and Phase_B differences angle in degrees are;

$$\frac{\Delta t_1}{T} * 360 = \frac{6.7 \text{ ms}}{20 \text{ ms}} \approx 120.6° \tag{4.4}$$

,and Phase_B and Phase_C differences angle in degrees are;

$$\frac{\Delta t_2}{T} * 360 = \frac{6.6 \text{ ms}}{20 \text{ ms}} \approx 118.8° \tag{4.5}$$

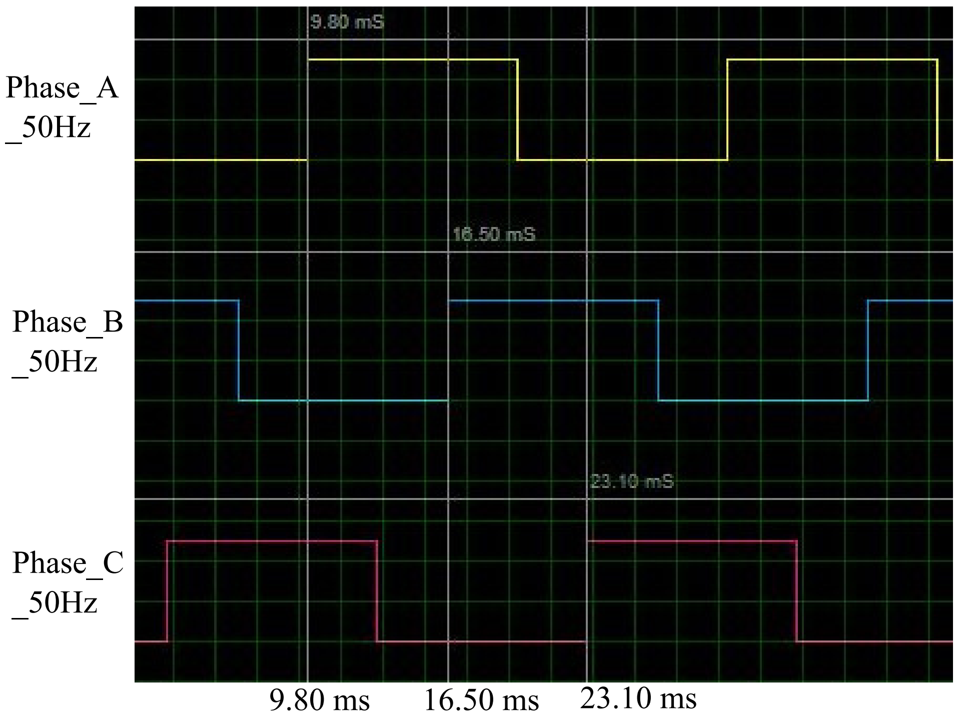

Figure 4.5 Simulation scope results of phase differences for phase A, B and C

As shown in Figure 4.6, actual scope results of Phase A and B to verify the simulation results in Figure 4.5. It’s clear that the difference is 6.68 ms between two reference edges in Figure 4.6.

In real time axis, the first edge reference time is 9.74 ms and the second edge reference time is 16.42 ms. The time difference can be calculated as;

$$\Delta t = 16.42 \text{ ms} - 9.74 \text{ ms} = 6.68 \text{ ms} \tag{4.6}$$

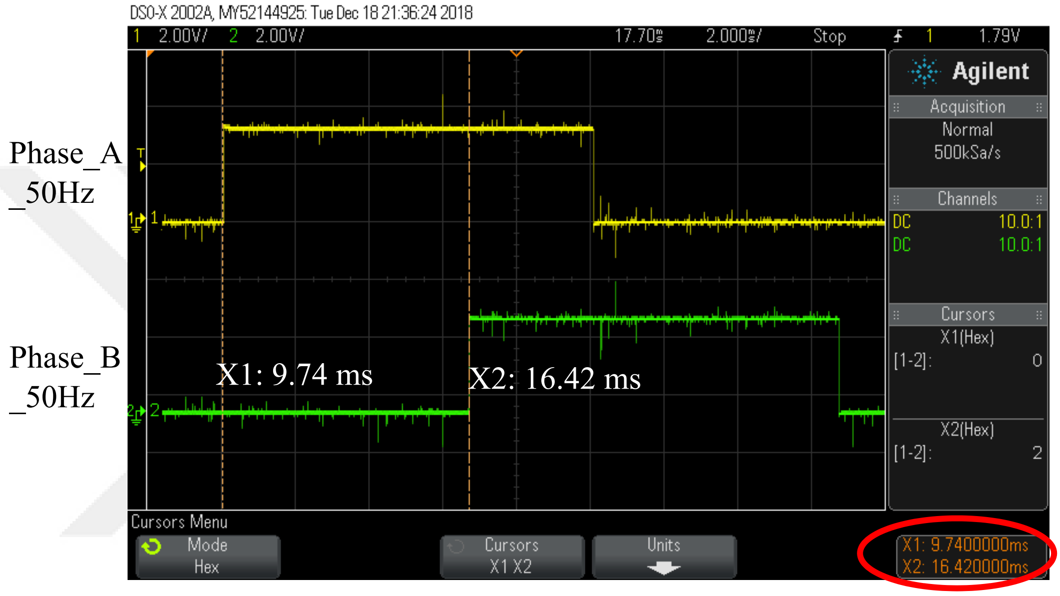

Figure 4.6 Actual scope results of phase differences for phase A and B

Figure 4.7 displays the pin number and name and Figure 4.5 shows the 120˚ phase difference between the green and the blue colored signals. The waveforms have been obtained after connecting one channel of the oscilloscope to the output of the buffer connecting pin PH6 from the microcontroller (Phase_A_50Hz) and the second channel has been connected to the output of the buffer connecting pin PB4 from the microcontroller (Phase_B_50Hz). The two waveforms have a phase difference of 120˚, same frequency and duty cycle of 50%.

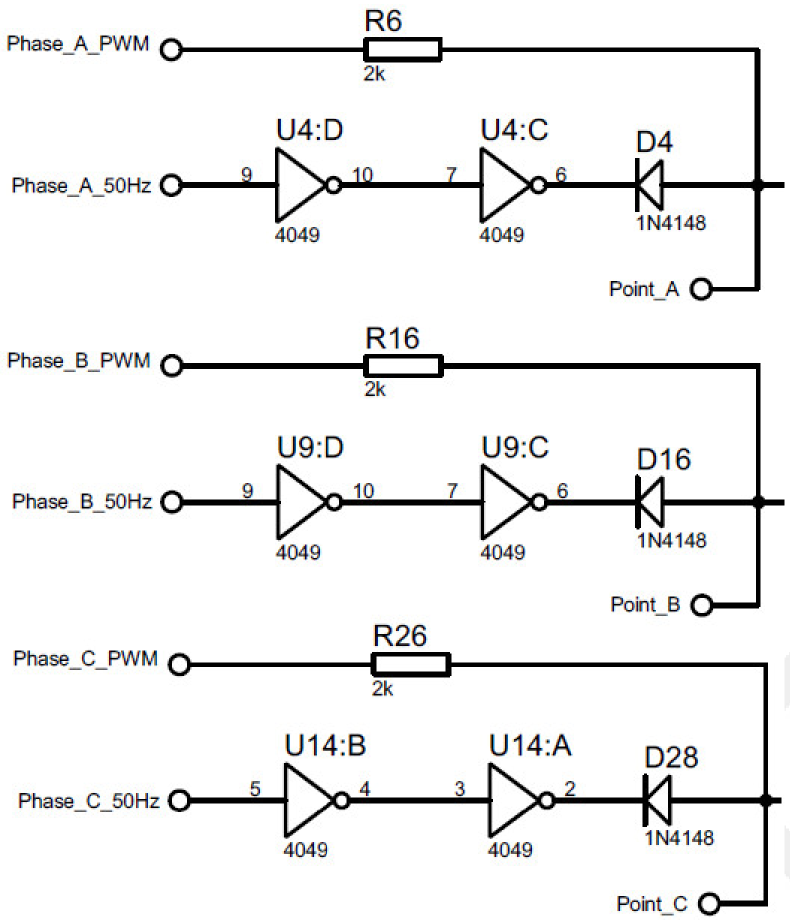

Figure 4.7 Circuit diagram of PWM and SPWM signals

Figure 4.8 shows that actual scope results of SPWM for Phase_A and Phase_B. It's clear that there is phase differences with some blank point positions. The time difference is nearly close to the calculated value in Equation 4.2 and 4.3.

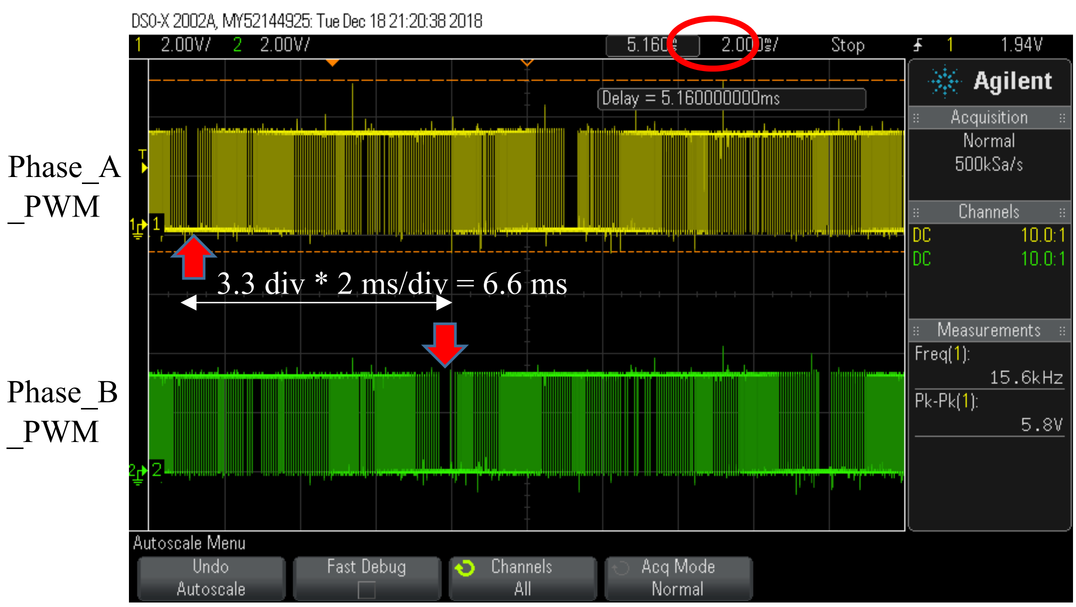

Figure 4.8 Actual scope results of SPWM for phase A and B

4.1.3 Dead Time Implementation

Generally, mosfet's turn off time is more slowly than their turn on time. If high-side of mosfet driver turns on and at the same time low-side of mosfet driver tırm off, (or vice versa), it may cause a damage due to the turning on at the same instant. This fault called by "shoot-through" condition which is detailed in Chapter 2.6. This condition may lead to damage of the components [17].

The reason for this undesirable case, one of the important ability of IR2112 mosfet driver is protection of the device itself against transients that may damage the circuit components. IR2112 mosfet driver has been used in this project does not have built-in or internal optocoupler or isolation component, hence it does not provide for "dead band" which is much needed in order to avoid short circuiting on the battery. Therefore, dead band has been applied to the circuit via externally shoot-through circuit.

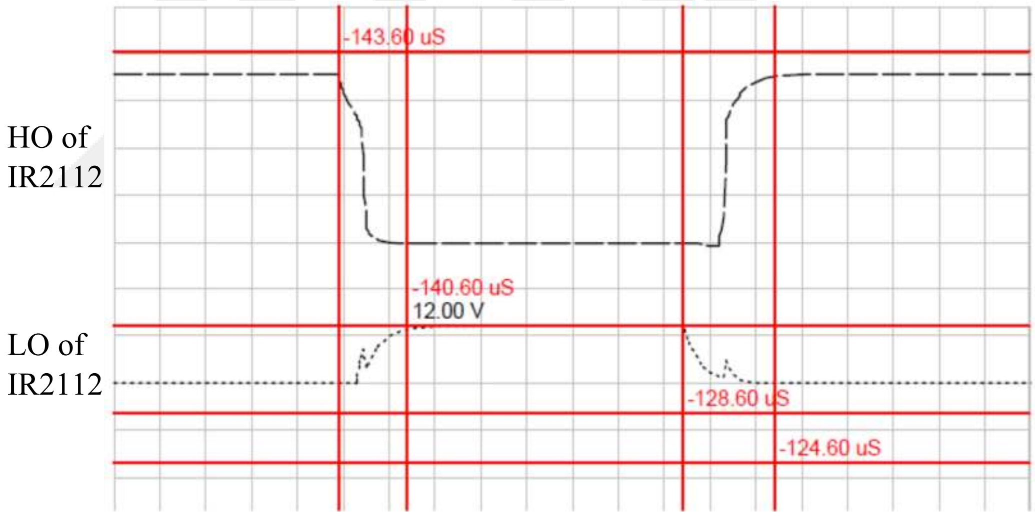

Figure 4.9 Dead band for gate signals of mosfets

Figure 4.9 shows that the simulation results of dead time in Proteus. The first time difference between turn off time of HS mosfet and turn on of LS mosfet is about 3 µs. Moreover, the second time difference between the turn on time of HS mosfet and turn off of LS mosfet is about 4 µs. HO and LO pins are specified in Figure 4.12 as pin numbers 1 and 7.

Figure 4.10 shows that the actual results of dead time. There is a little time differences between the actual & simulated results.

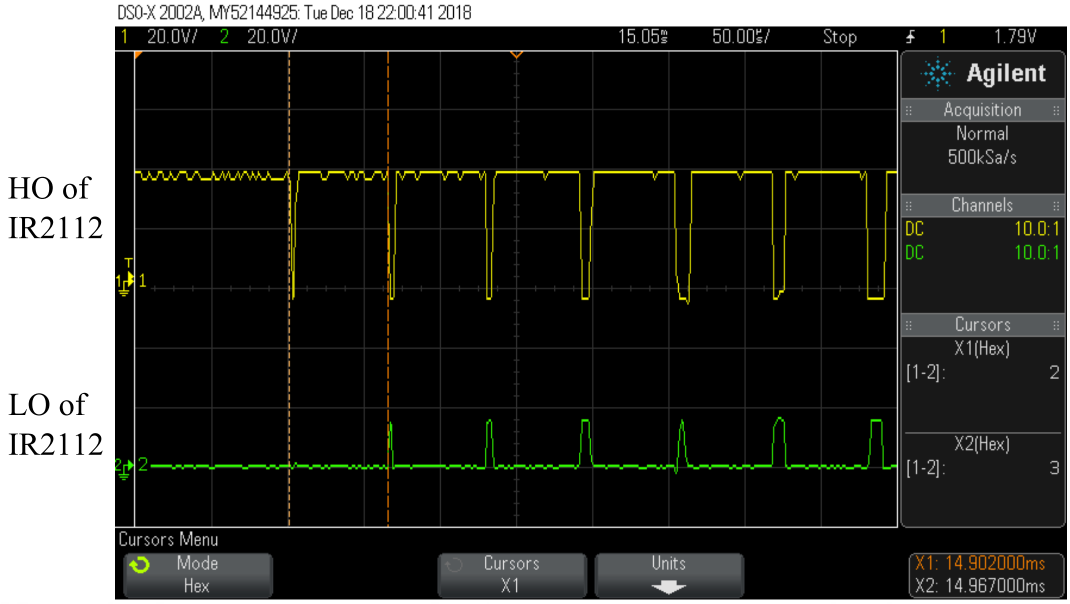

Figure 4.10 Actual scope results of dead time

$$\text{Dead Time} = 14.967 \text{ ms} - 14.902 \text{ ms} = 65 \text{ µs} \tag{4.7}$$

HO and LO pins are specified in Figure 4.12 as pin numbers 1 and 7.

4.1.4 Mosfet Driver Inputs

As shown in Figure 4.11, Left_HIN and Left_LIN are inputs of left side mosfet driver, Right_HIN and Right_LIN are inputs of right side mosfet driver as well. These control signals have been operated in digital logic level.

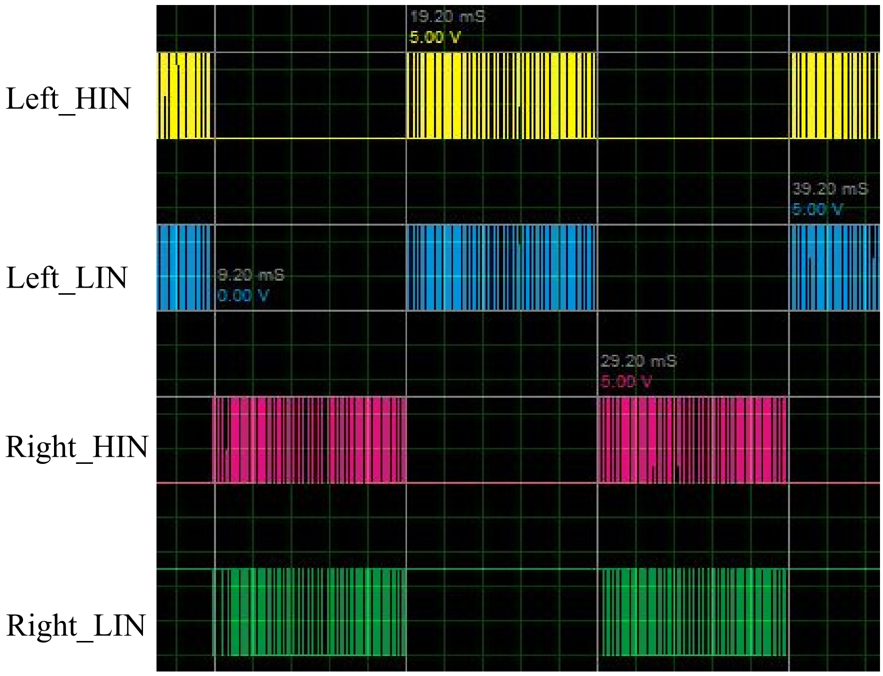

Figure 4.11 Simulation scope results of mosfet driver input signals

Figure 4.12 shows the left side of H-bridge mosfet driver. Also, Figure 4.13 shows the right side of H-bridge mosfet driver. The pin number 10 is high side input and 12 is low side input.

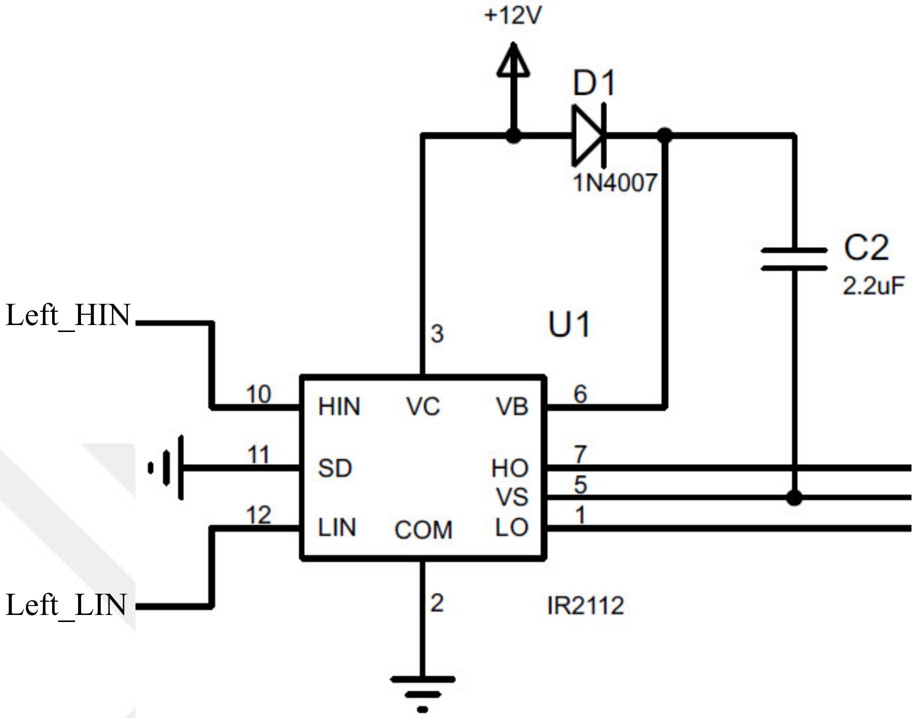

Figure 4.12 Left-side of H-bridge mosfet driver

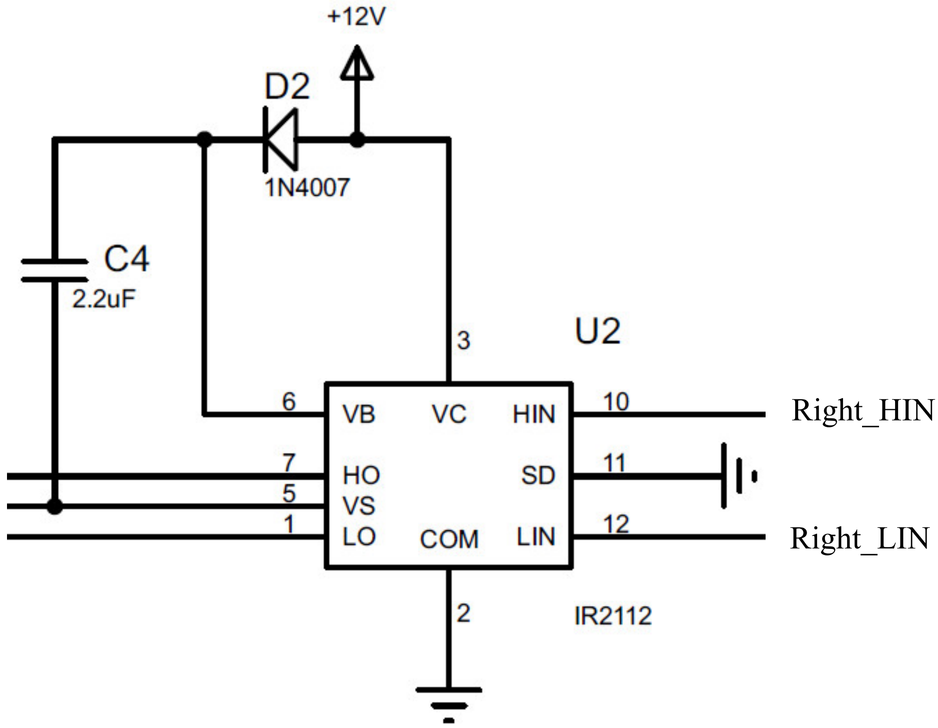

Figure 4.13 Right-side of H-bridge mosfet driver

4.1.5 Mosfet Driver Outputs

As shown in Figure 4.15 and Figure 4.16, gate signals of mosfets are connected to mosfet driver outputs. D9, D10, D11 and D12 discharge the gate capacitances of mosfet quickly, bypassing the gate resistors, reducing the turn off time. R1, R2, R3 and R4 are the gate current-limiting resistors.

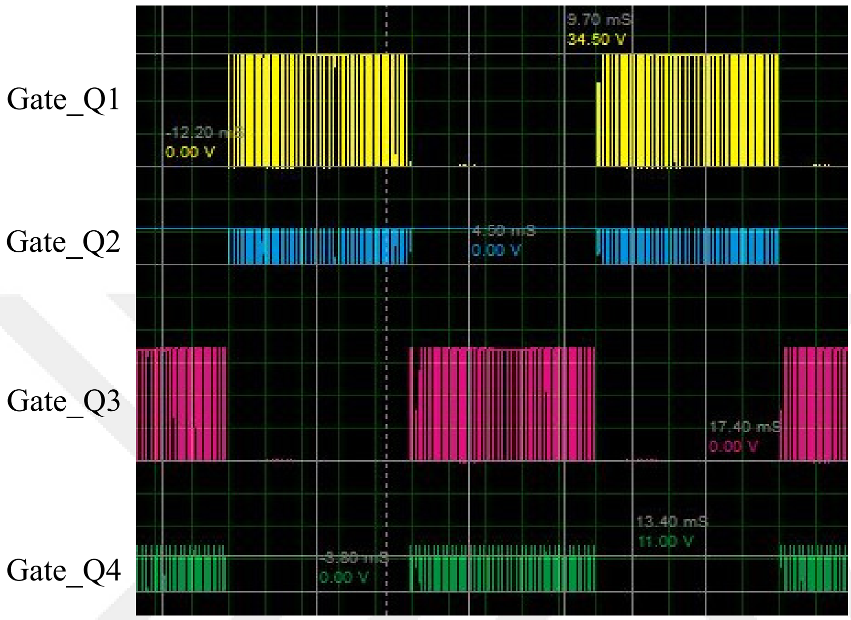

Figure 4.14 Gate signals of mosfets

As shown in Figure 4.14, Gate_Q1 and Gate_Q3 are high-output, Gate_Q2 and Gate_Q4 are low-output. High side outputs peak value is greater than Low side outputs peak value due to supply offset voltage V_s.

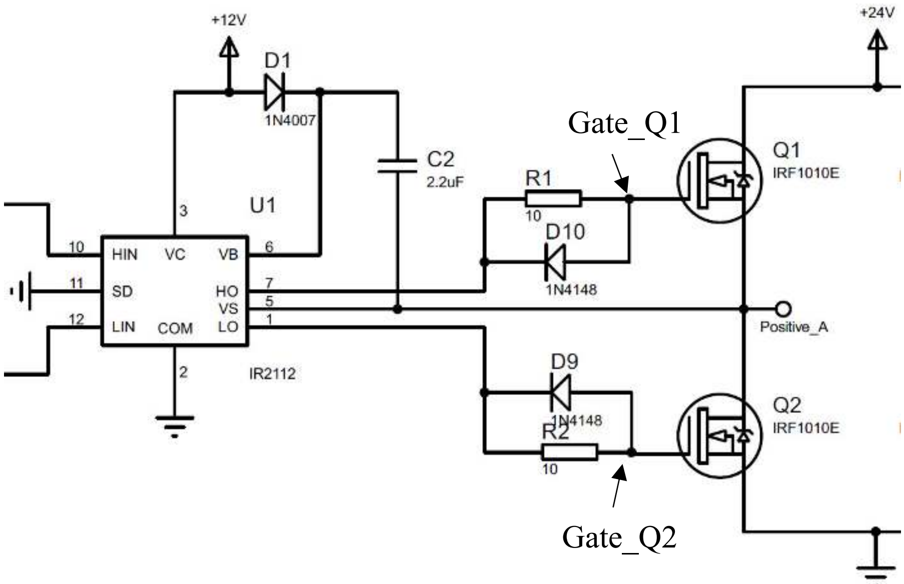

Figure 4.15 Left side mosfer driver circuit

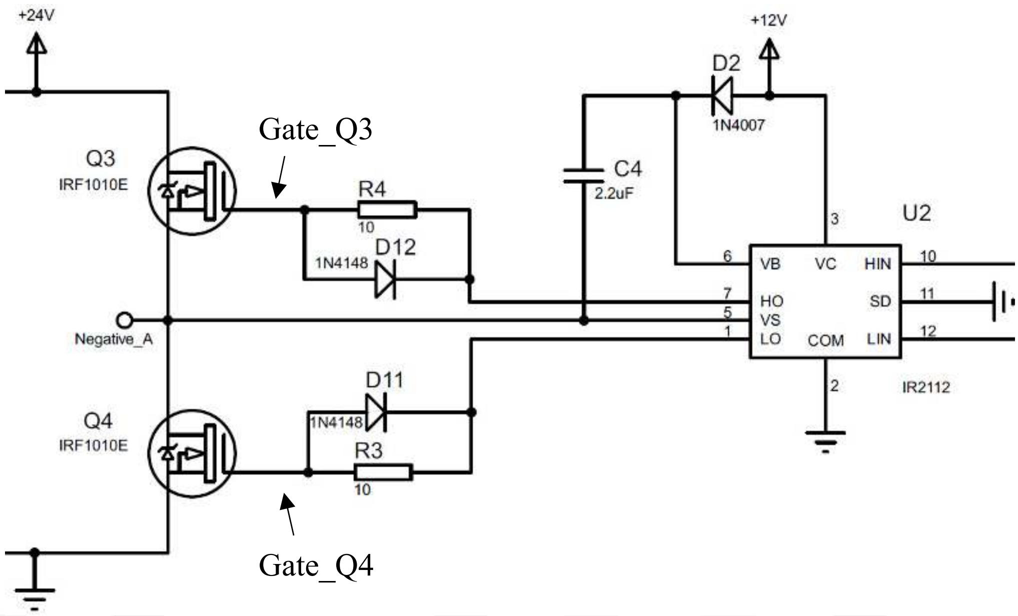

Figure 4.16 Right side mosfer driver circuit

4.1.6 H-Bridge Output

As shown in Figure 4.17, left side and right side has been summed as H-Bridge Output in simulation. Also, this output is primary input side of step-up transformer.

In Figure 4.15, Positive_A shows H bridge left side common point. In Figure 4.16, Negative_A shows H bridge right side common point.

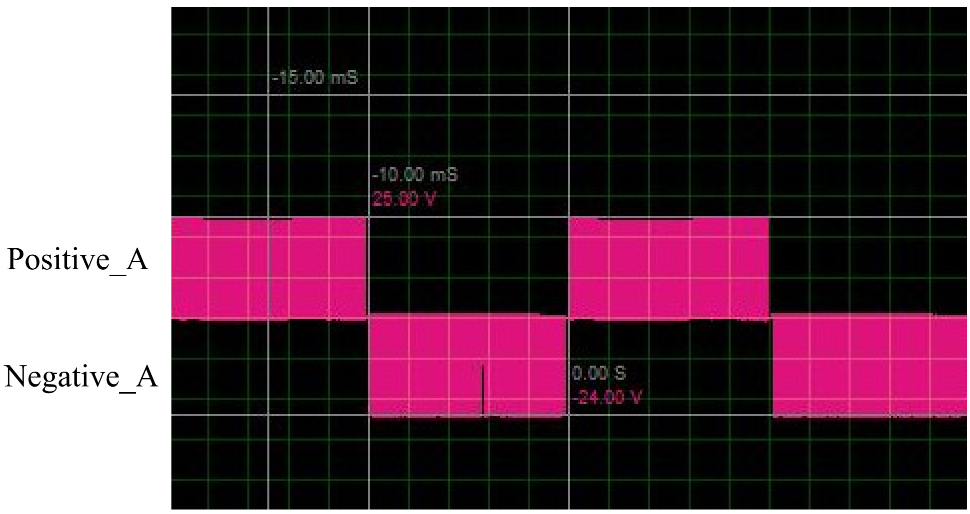

Figure 4.17 H bridge output simulation results

4.2 Filtered Output

In circuit theory, to get a pure sine wave at the output, it is required a filter which can cancel all the excess frequencies above cut-off frequency [18].

Basically, a filter can not insert new frequencies to the input signal, nor can not modify the component frequencies of that signal, but it can modify the relative amplitudes of the various frequency components and/or their phase relationships. The frequency-domain behavior of a filter is described mathematically in terms of its transfer function or network function. This is the ratio of the Laplace transforms of its output and input signals. The voltage transfer function H(s) of a filter given by [19]:

$$H(s) = \frac{Vout(s)}{Vin(s)} \tag{4.8}$$

The circuit below in Figure 4.18 shows a low pass filter. This LC filter passes low frequency signals. However, it cancels signals at frequencies above the filter's cutoff frequency. The transfer function of the filter circuit is given by;

$$H(s) = \frac{\frac{1}{LC}}{s^2 + \frac{1}{LC}} \tag{4.9}$$

Standart 2nd order equation is given by;

$$T(s) = \frac{w_C^2}{s^2 + w_C^2} \tag{4.10}$$

Cut-off frequency is given by;

$$w = \frac{1}{\sqrt{LC}} \tag{4.11}$$

$$f_C = \frac{1}{2\pi\sqrt{LC}} = \frac{1}{2\pi\sqrt{12 * 10^{-3} * 20 * 10^{-6}}} \approx 325 \text{ Hz} \tag{4.12}$$

As shown in Figure 4.18, step-up transformer and LC filter parameters are given which is calculated in Equaiton 4.12.

The objective of this step is to make the critical frequency as close as possible to the required frequency 50 Hz.

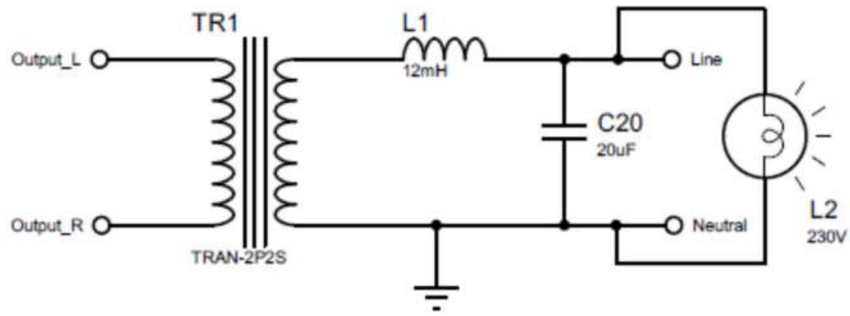

Figure 4.18 Step-up transformer and LC filter

As shown in Figure 4.19, unfiltered mosfet output of left side's peak value is +24 V DC. However, unfiltered mosfet output of right side's peak value is -24 V DC. Theoretically, 220 V AC in rms means 311 V peak value because of sine wave. Therefore, transformer turn ratio is expressed as 13 in Equation 4.13.

$$\text{Transformer Turn Ratio} = \frac{311\ V_{peak}}{24\ V_{peak}} \approx 13 \qquad (4.13)$$

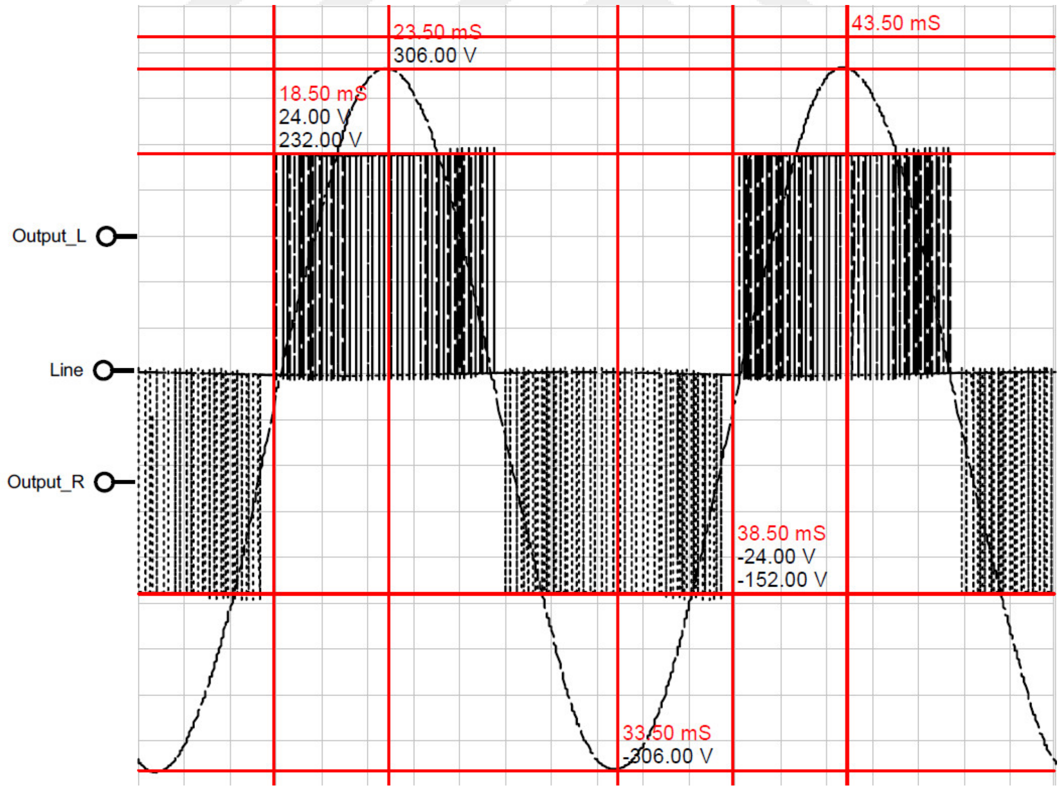

Figure 4.19 Unfiltered mosfet output and filtered sine wave

CHAPTER 5

RESULTS AND ANALYSIS

5.1 Connection of Power Quality Analyzer

As shown in Figure 5.1, connection diagram has been applied to 3-phase inverter.

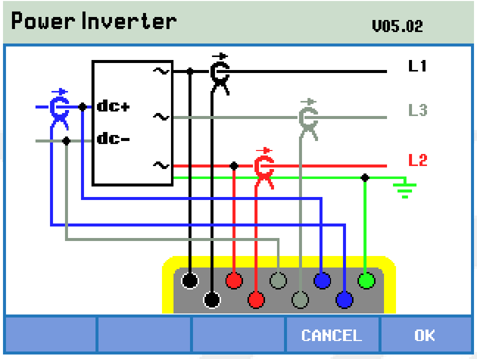

Figure 5.1 Connection diagram of Fluke 435-II power quality analyzer

Fluke 435-II Power Quality Analyzer has been used for measurements which are voltage, current, scope results of phase, phase vector diagram.

5.2 Inverter Test under No-Load Condition

Figure 5.2 shows that H-bridge output scope view in simulation before filter and step-up transformer. Unfiltered SPWM output's peak value is 24 V. After filter, pure sine wave's peak value is 308 V.

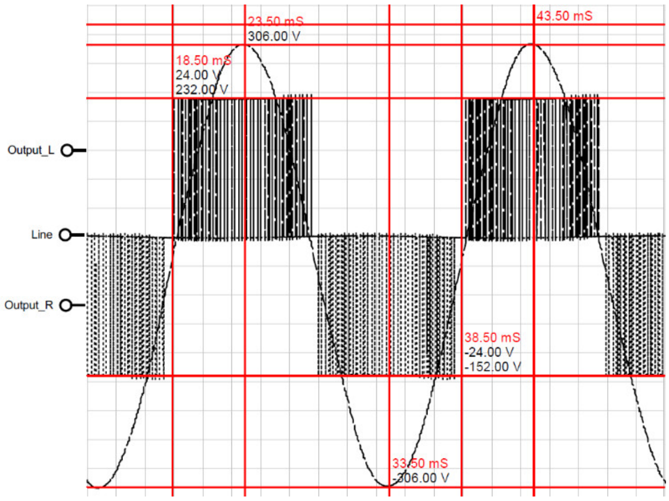

Figure 5.2 Simulation scope result of sine wave under no-load condition

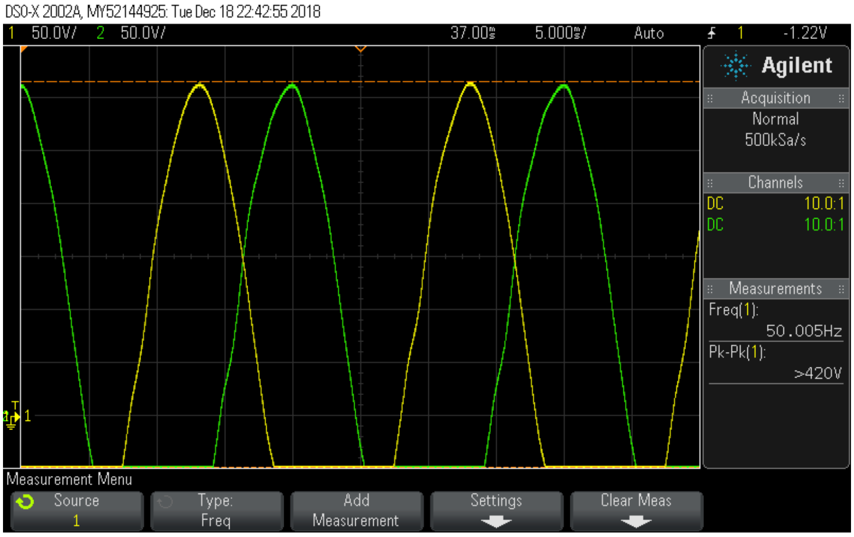

Figure 5.3 Actual results of 2-sine wave positive cycle under no-load condition

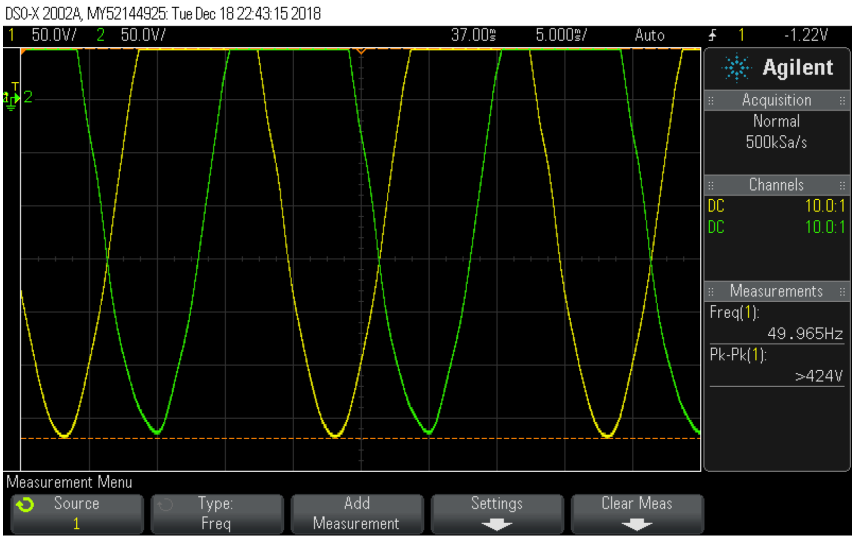

Figure 5.4 Actual results of 2-sine wave negative cycle under no-load condition

Figure 5.3 and Figure 5.4 shows that actual scope results of pure sine wave recorded at the output. The peak value of sine wave is about 310 V. It is so close to simulation results which was 308 V.

As shown in Figure 5.3 and 5.4, the full sine wave has not been fitted to the full screen due to the probe multiplication factor. Normally, oscilloscope's maximum voltage division ratio is 50 V/div. Under test conditions, peak value is +311 V in positive cycle, -311 V in negative cycle. Therefore, 622 V peak-to-peak value is required for measurement in full screen. However, this oscilloscope has 8 square with 50 V/div, so maximum value can be measured as 400 V. That's why, it has been measured in two parts in negative and positive cycle.

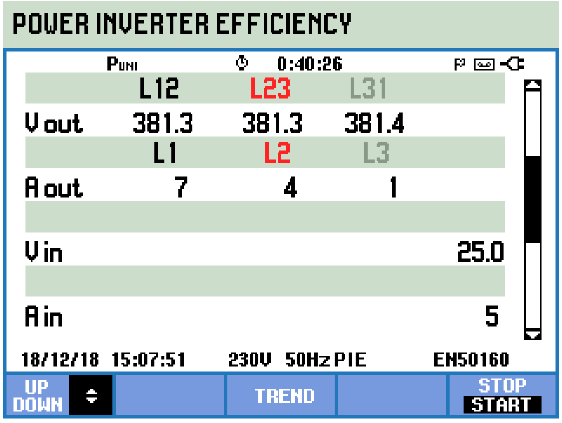

Figure 5.5 Phase-phase voltage measurement under no-load condition

As shown in Figure 5.5, phase-to-phase voltage is about 381 V for between each phase in no-load condition measured by Fluke 435-II Power Quality Analyzer.

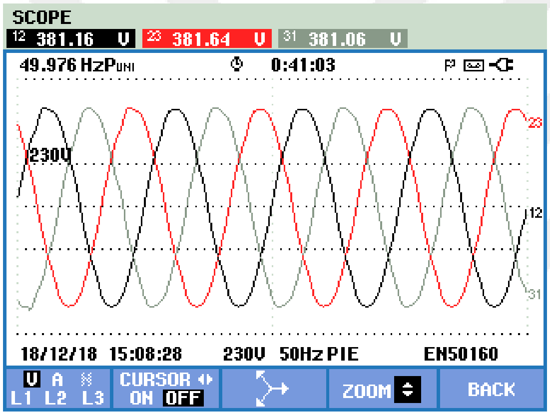

Figure 5.6 3-phase sine wave scope results under no-load condition

As shown in Figure 5.6, black colored sine wave represents the first phase voltage, gray colored sine wave represents the second phase voltage and red colored sine wave represents the third phase voltage. All of these sine wave in 49.976 Hz in real results.

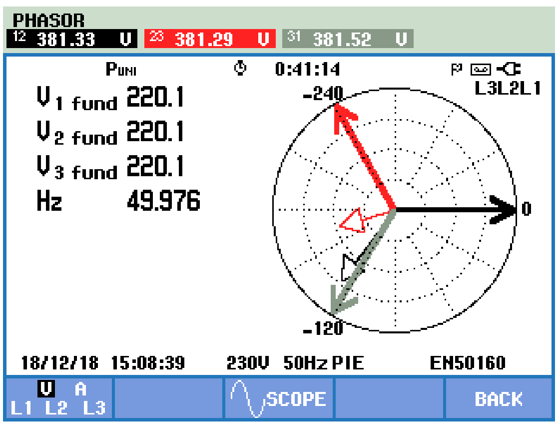

Figure 5.7 3-phase vector diagram under no-load condition

As shown in Figure 5.7, vector diagram has been presented by Fluke 435-II Power Quality Analyzer. Also, it is clear that the voltage between line-to-neutral is about 220 V.

Table 5.1. Actual measurement of 3-phase inverter under no-load condition

Battery Voltage	Current from Battery	AC Voltage between Line-Neutral	Ouput AC Current
V_{DC}	I_{DC}	V_{L-N}	I_{AC}
25.05 V	1.4 A	220 V	0 A

Inverter power idle consumption is given by;

$$P_{IDLE} = V_{DC} * I_{DC} = 25.05\ V * 1.4\ A = 35.07\ W \tag{5.1}$$

5.3 Inverter Test under Load Condition

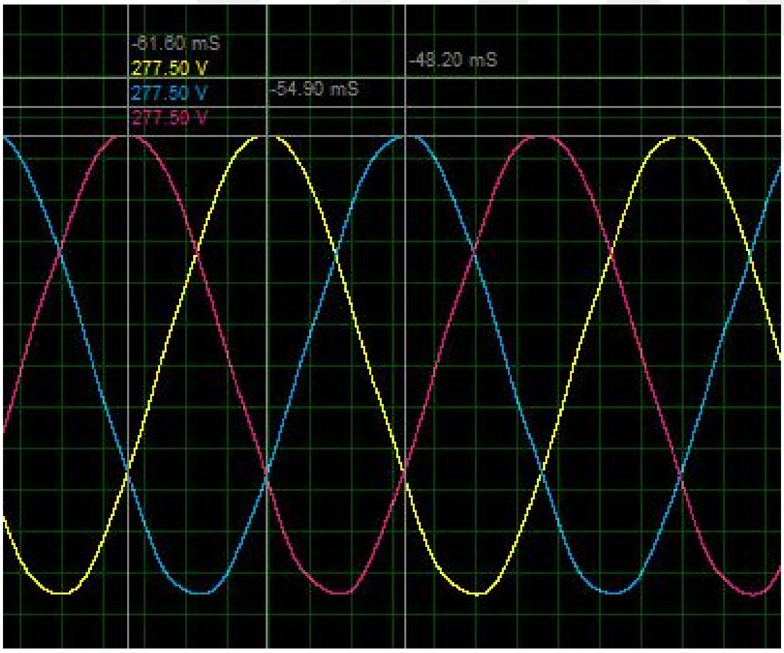

Figure 5.8 Simulation scope result of 3-sine wave under resistive load condition

As shown in Figure 5.8, resistive load condition has been simulated in Proteus. The peak value of sine wave is 277.5 V. The RMS value is calculated by;

$$V_{RMS} = \frac{V_{peak}}{1.414} = \frac{277.5\ V}{1.414} = 196.25\ V \tag{5.2}$$

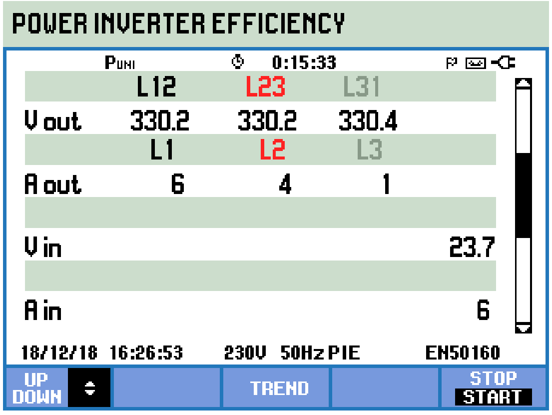

Figure 5.9 Phase-phase voltage measurement under load condition

As shown in Figure 5.9, phase-to-phase voltage is about 330 V for between each phase in full resistive load condition measured by Fluke 435-II Power Quality Analyzer.

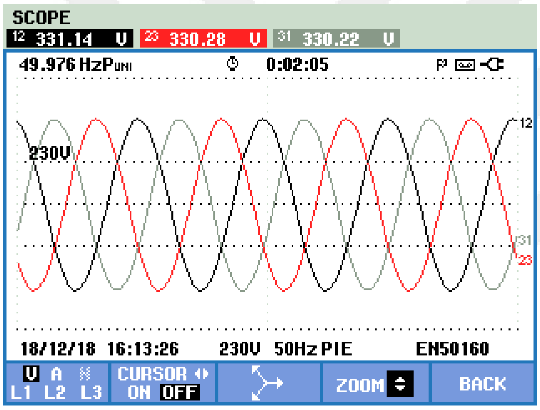

Figure 5.10 3-phase sine wave scope results under load condition

As shown in Figure 5.10, black colored sine wave represents the first phase voltage, gray colored sine wave represents the second phase voltage and red colored sine wave represents the third phase voltage. All of these sine wave in 49.976 Hz in real results.

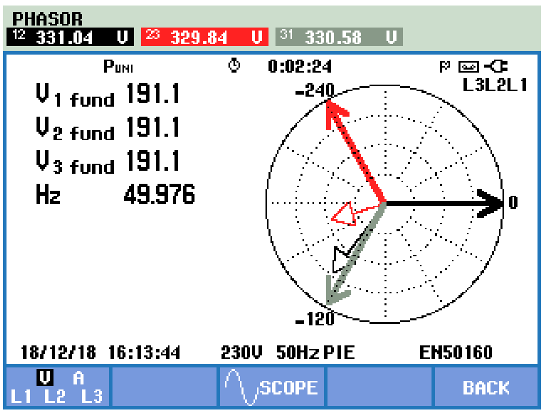

Figure 5.11 3-phase vector diagram under load condition

As shown in Figure 5.11, vector diagram has been presented by Fluke 435-II Power Quality Analyzer. Also, it is clear that the voltage between line-to-neutral is about 191 V. The current from battery has been measured by DC ampermeter and output current has been measured by AC ampermeter which is expressed in Table 5.2. The resistive load is Y connected 3x160 W lamp.

Table 5.2. Actual measurement of 3-phase inverter under load condition

Battery Voltage	**Current from Battery**	**AC Voltage between Line-Neutral**	**Ouput AC Current**
V_{DC}	I_{DC}	V_{L-N}	I_{AC}
23.7 V	15.7 A	191.1 V	0.579 A

Input DC power consumption with resistive load conditions given by;

$$P_{Input} = V_{DC} * I_{DC} = 23.7\ V * 15.7\ A = 372.09\ W \tag{5.3}$$

Output AC power with resistive load conditions given by;

$$P_{output} = 3 * V_{AC} * I_{AC} = 3 * 191.7\ V * 0.579\ A = 332.98\ W \tag{5.4}$$

Inverter efficiency with resistive load given by;

$$\eta = \frac{P_{output}}{P_{input}} = \frac{332.98\ W}{372.09\ W} = \%89.49 \tag{5.5}$$

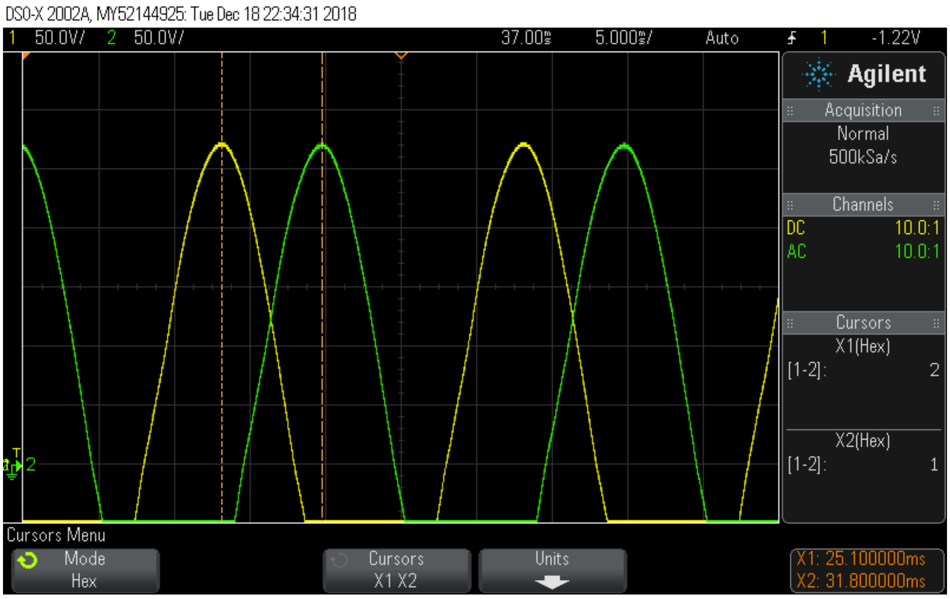

Figure 5.12 Actual results of 2-sine wave positive cycle for no-load condition

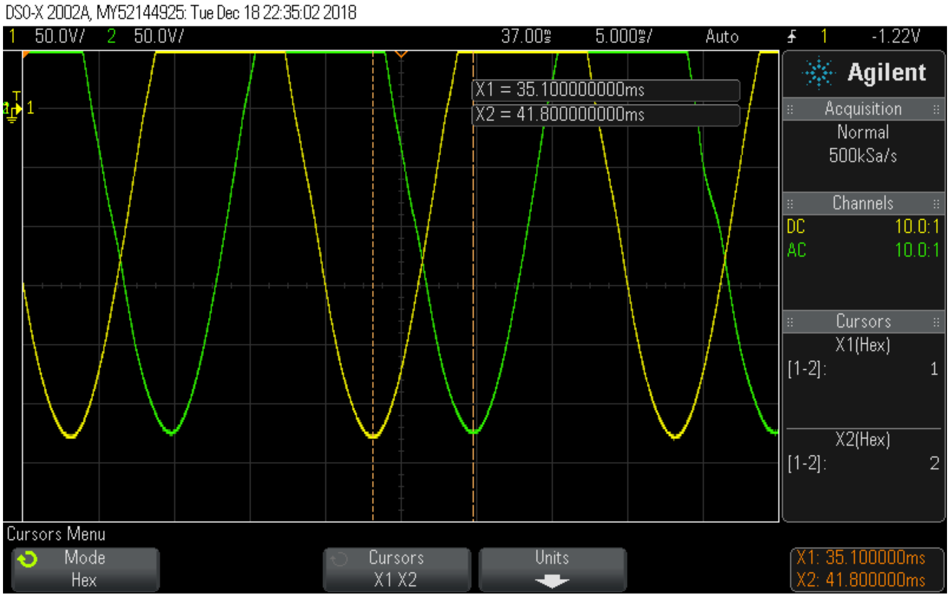

Figure 5.13 Actual results of 2-sine wave negative cycle under no-load condition

As shown in Figure 5.13, Phase 1 and Phase 2 are measured by oscilloscope at the same time. It's clear that the time difference between two peak point of sine wave is 6.7 ms (41.8 ms – 35.10 ms) This value is verified with simulation value in Chapter 4.1.2.

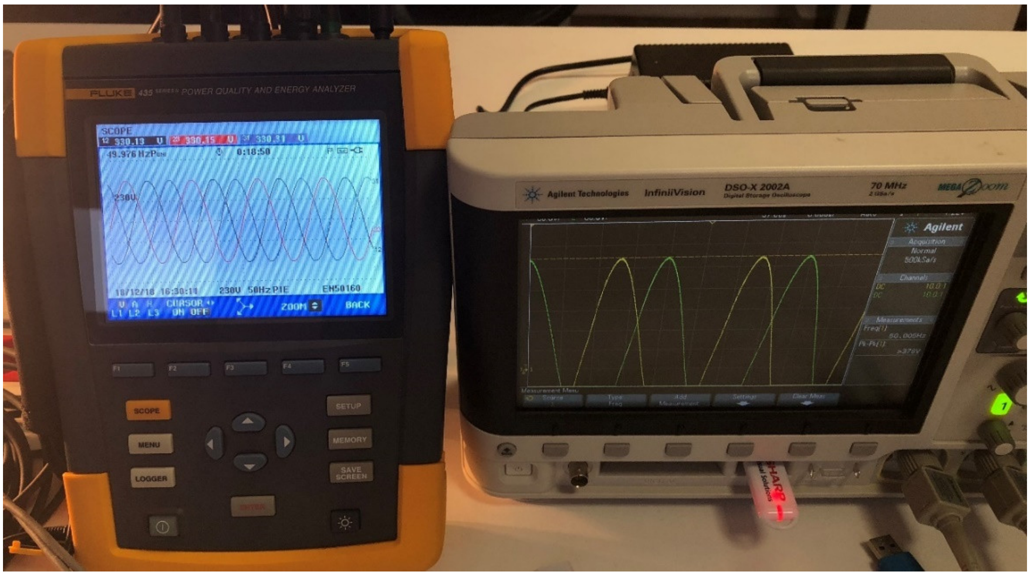

Figure 5.14 Actual measurement of 3-phase ınverter

Figure 5.14 shows that the real time measurement of three-phase inverter with Agilent oscilloscope and Fluke 435-II Power Quality Analyzer.

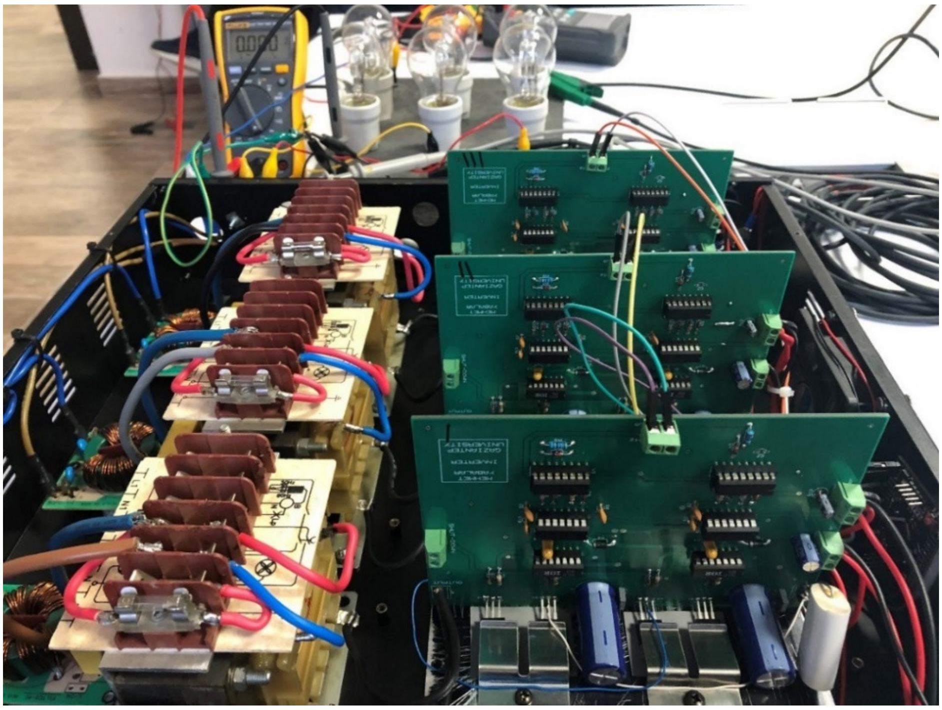

Figure 5.15 3-phase inverter side-view

Figure 5.15 and 5.16 shows that three-phase inverter which has 3 transformer, 3 LC filter, 3 driver board and heatsink. There are two snubber capacitor on the DC Bus bar. The first capacitor is so close to input side of battery cable, the second capacitor is so close to end of Bus bar to barrier rush currents due to the suddenly turn-on and off.

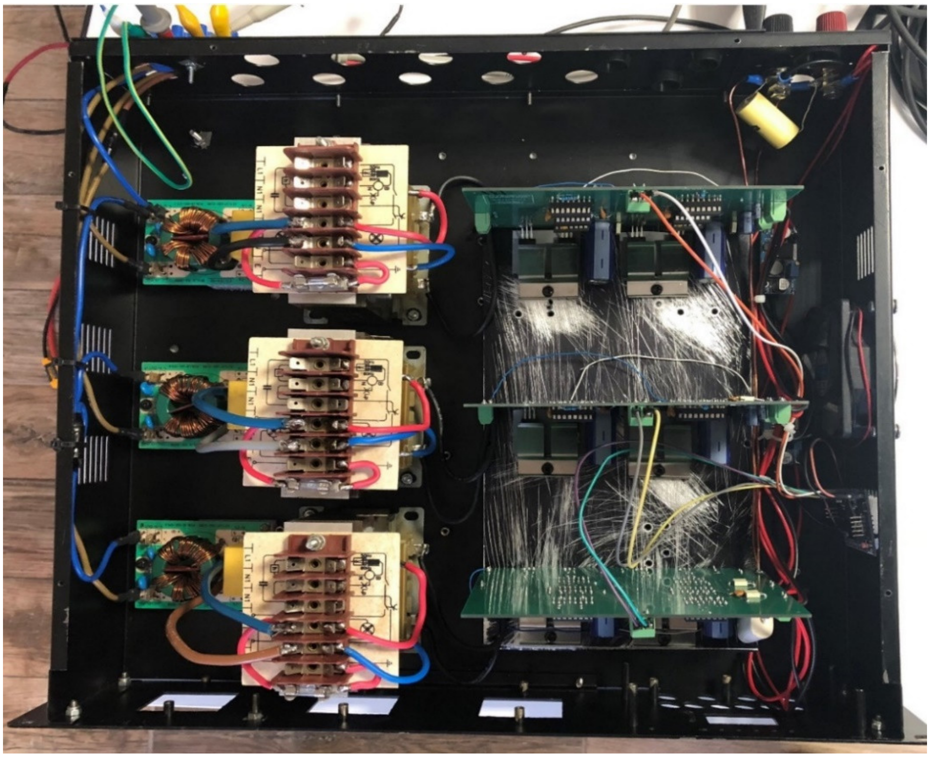

Figure 5.16 3-phase inverter top-view

CHAPTER 6

CONCLUSION AND RECOMMENDATIONS

6.1 Conclusion

The power electronics devices are getting smaller, consequently the efficiency of inverter should be improved. The different switching methods and components have been used in microcontroller based three phase SPWM inverter. Based on this research, SPWM method is a well-known method used in inverter circuits. The simulation of the three-phase inverter device model is simulated in Proteus and hardware implemented.

The frequency of the output voltage has been measured as 49.976 Hz. The desired output frequency is 50 Hz and the difference can be attributed to execution time, propagation delay of the varios components used and 8-bits microcontroller. It can be solved with using 16 or more bits microcontroller.

The output voltage has been decreased when load is connected because of open-loop system. There is no feedback system, therefore the efficiency can vary with load conditions. As shown in equality 5.5, the efficiency has been calculated as nearly %90. This efficiency is so close to the inverter which has same power and voltage on the market. According to the appendix D parts list, this new designed inverter is cheaper than inverter on the market [20].

The inverter has not been tested by any motor loads. That is why the voltage driven inverter does not operate satisfactorily on motor loads. At the time of startup, power requirements of a motor may be several times more than required in the normal operation. This extreme transient condition may continue for several seconds depending on the angular acceleration of the motor's rotor. Moreover, the power factor of the motor at this condition becomes extremely low and may be of the order 0.2 lagging. Even with a power factor improvement capacitor connected across the motor, the low transient power factor during start-up cannot be compensated. To cater for transient power, the rating of the semiconductor devices and the transformer should be adequately increased and properly protected. Alternatively, the motor inrush current could be restricted to a minimum value by inserting a current-limiting resistor in series with the motor. The loop response should be compatible with the motor, otherwise there will be hunting. That is sudden application or removal of motor load may generate oscillations which may continue indefinitely if a proper damping arrangement is not provided [21].

6.2 Recommendations for Future Work

Basically, this project has been designed without any feedback. Therefore, this design is an open-loop system. The problem is voltage output can be changed depends on how much load connected to the output. The output voltage may be decreased by increasing load. The output voltage of inverter must be regulated by independently from load. That's why it is needed a feedback control system. This feedback system would give the micrcontroller a measurement of the output across the load, so that the signals controlling the system may be adjusted according to precise parameters in the programming code.

Another recommendation is implementing a PFC (Power Factor Correction) circuit like voltage boost converter which can decrease the effect battery voltage drop on the output. DC/DC boost converter can step up the battery voltage from 24 V_{DC} to 340 V_{DC}. Normally, 311 V_{DC} is the peak value of 220 V_{AC}. However, there is some switching losses and 90% duty cycle for protection. It's required to use 340 V_{DC} instead of 311 V_{DC}.

REFERENCES

[1] S. Hannan, S. Aslam ve M. Ghayur. (2018). Design and real-time implementation of SPWM based Inverter. *International Conference on Engineering and Emerging Technologies (ICEET).* **10**, 1-6.

[2] P. C. SEN. 1987. Power Electronics Rajkamal Electric. Karnal: TATA McGRAW-HILL Publishing Company.

[3] S. Phogat. (2014). Analysis of Single-Phase SPWM Inverter. *International Journal of Science and Research (IJSR).* **3**,1793-1798.

[4] B. Majhi. (2012). Analysis of Single-Phase SPWM Inverter. *National Institute of Technology, Rourkela.* **1**, 5-27.

[5] University of Technology Department of Laser and Optoelectronics Engineering. 2011. Multi Pulse Width Modulation Techniques (MPWM). Exp:14.

[6] National Institute of Technology Rourkela. 2012. Modified Sinusoidal Pulse Width Modulation (SPWM) Technique Based Controller. http://shodhganga.inflibnet.ac.in/ bitstream/10603/33606/10/10_chapter5.pdf., 16.01.2019.

[7] Muhammad. H. Rashid. 2003. Power Electronics Circuits, Devices, and Applications. 3th Edition. Prentice Hall: Pearson.

[8] Worcester Polytechnic Institute. 2006. DC/AC Pure Sine Wave Inverter. https://web.wpi.edu/Pubs/Eproject/Available/Eproject042507092653/unrestrict/MQP_D_1_2.pdf., 16.01.2019

[9] Dongjie Cheng. 2008. Add Fail-Safe Shoot-Through Protection To Power MOSFET. https://www.electronicdesign.com/electromechanical/add-fail-safe-shoot-through-protection-power-mosfet. 16.01.2019.

[10] Modular Circuits. 2012. Shoot-Through Protection. http://www.modularcircuits.com/blog/articles/h-bridge-secrets/h-bridge-control/., 16.01.2019.

[11] Texas Instruments Unitrode Application Note. 1999. Practical Considerations in Current Mode Power Supplies. U-111.

[12] International Rectifier. 2007. Application Note. AN-978. HV Floating MOS-gate driver ICs. 6. p. California

[13] International Rectifier. 2005. IR2112 High and Low Side Driver Datasheet PD60026. California

[14] Texas Instruments Application Note. 2012. SM72295 Highly Integrated Gate Driver for 800VA to 3kVA Inverter. 2. p. AN-2296.

[15] Texas Instruments Application Note. 2012. SM72295 Highly Integrated Gate Driver for 800VA to 3kVA Inverter. 3. p. AN-2296.

[16] University of Nairobi Faculty of Engineering. 2014. Microcontroller Based Power Inverter. 30. p. Nairobi.

[17] Muhammad. H. Rashid. 2003. Power Electronics Circuits, Devices, and Applications: Shoot-Through Circuit. 3th Edition. Prentice Hall: Pearson. 240 p.

[18] John Bird. 2003. Electrical Circuit Theory and Technology. 2nd Edition. Oxford. Newnes an Imprint of Elsevier Science.

[19] National Semiconductor Application Note. 1991. A basic introduction to filters-active, passive and switched capacitors. AN-779.

[20] COTEK icmaster. 2018. 600W Pure Sine Wave Inverter. http://www.icmaster.com.hk/PDF/COTEK%20%20%2003-6062-C110.pdf. 16.01 2019.

[21] University of Nairobi. 2004. Microcontroller Based Three Phase Inverter. http://eie.uonbi.ac.ke/sites/default/files/cae/engineering/eie/MICROCONTROLLER%20BASED%20THREE%20PHASE%20INVERTER.pdf

[22] S. Maheshri ve P. Khampariya. (2017). Simulation & Hardware Development of Single Phase Sinusoidal Pulse Width Modulation (Unipolar) Inverter. *International Journal on Recent Technologies in Mechanical and Electrical Engineering (IJRMEE)*. **6**. 4102-4108.

[23] J. Sanchez, M. P. Canton. 2009. Microcontroller Programming the microchip pic. 1st Edition. Florida, USA: CRS Press.

APPENDIX

Appendix A: Arduino Mega 2560 Code

```
/*
 * Arduino ATMEGA2560 Board....
 * Three Phase Sine Wave PWM Generation
 * Each Phase is 120 degree out of Phase
 * PWM is for 50Hz sine wave
 * Sine Lookup Table is used for generating PWM
 * Contains 50 samples in 90 degree
 */
#define F100_1 22      ///50Hz wave for Phase_A
#define F100_2 23      ///50Hz wave for Phase_B
#define F100_3 24      ///50Hz wave for Phase_C
unsigned char PWM_Duty_Cycle = 0;          //Phase_A PWM Duty Cycle
unsigned char PWM_Duty_Cycle1 = 33;        //Phase_B PWM Duty Cycle
unsigned char PWM_Duty_Cycle2 = 33;        //Phase_C PWM Duty Cycle
unsigned char SinLkUpTab[1][50]= {0, 7, 14, 22, 29, 36, 43, 50, 57, 64, 71, 78, 85, 91, 98, 104, 111,
117, 123, 129, 135, 141, 147, 152, 157, 163, 168, 173, 177, 182, 186, 190, 194, 198, 202, 205, 208, 211,
214, 216, 219, 221, 223, 224, 226, 227, 228, 229, 230, 230};
///SINE WAVE LOOKUP TABLE OF 50 ENTRIES///
unsigned char Count = 0,Count1 = 3,Count2 = 7, MSec10 = 0, MSec101 = 3,MSec10_2 = 6,MSec = 0;
unsigned char counter1=0;
unsigned int counter=0;

void setup()
{
  //pinMode(ledPin, OUTPUT);
  pinMode(9,OUTPUT);            //SETTING PIN 9 AS OUTPUT
  pinMode(10,OUTPUT);           //SETTING PIN 10 AS OUTPUT
  pinMode(5,OUTPUT);            //SETTING PIN 5 AS OUTPUT
```

```
  pinMode(F100_1,OUTPUT);        //SETTING PIN 22 AS OUTPUT
  pinMode(F100_2,OUTPUT);        //SETTING PIN 23 AS OUTPUT
  pinMode(F100_3,OUTPUT);        //SETTING PIN 24 AS OUTPUT
  digitalWrite(F100_1, 0);       //WRITE 0 TO PHASE A 50HZ WAVE
  digitalWrite(F100_2, 1);       //WRITE 1 TO PHASE B 50HZ WAVE
  digitalWrite(F100_3, 0);       //WRITE 0 TO PHASE C 50HZ WAVE
  // INITIALIZE TIMER1 AND SET IT TO 100us INTERRUPT ////
  noInterrupts();                // DISABLE ALL INTERRUPTS
  TCCR1A = 0;
  TCCR1B = 0;
  TCCR2B = TCCR2B & 0b11111000 | 0x01;       //setting pin 9 and pin 10 frequency 31372.55Hz
  TCCR3B = TCCR3B & 0b11111000 | 0x01;       //setting pin 5 and pin 6 frequency 62500Hz
  TCNT1 = 65442;                             // preload timer 65536-16MHz/256/2Hz ...for 100us
  TCCR1B |= (1 << CS11);                     // 256 prescaler
  TIMSK1 |= (1 << TOIE1);                    // enable timer overflow interrupt
  interrupts();                              // enable all interrupts
}
////INTERRUPT SERVICE ROUTINE FOR GENERATING PWM SIGNALS//////
ISR(TIMER1_OVF_vect)
{
  TCNT1 = 65442;           //LOAD TIMER1 65442
  Count++;
  Count1++;
  Count2++;
  //digitalWrite(ledPin, digitalRead(ledPin) ^ 1);
  /////PHASE_A PWM BY USING 0C2B PWM PIN///////
   OCR2B = SinLkUpTab[0][PWM_Duty_Cycle];
   analogWrite(9,OCR2B);
     if(MSec10 < 5 ){
       if(PWM_Duty_Cycle < 49)
          PWM_Duty_Cycle++;
      }else{
      if(PWM_Duty_Cycle > 0)
```

```
    PWM_Duty_Cycle--;
   }
   ////////////////////
      if(Count >= 10){
  Count = 0;
  MSec = 1;
  MSec10++;
  //MSec101++;
  if(MSec10 == 10){
    MSec10 = 0;
    PWM_Duty_Cycle = 0;
    digitalWrite(F100_1, digitalRead(F100_1) ^ 1);    //INVERT 50Hz SIGNAL
  }
 }
////////////////////////////////////////
////////PHASE_B PWM BY USING 0C2A PWM PIN/////////
 OCR2A = SinLkUpTab[0][PWM_Duty_Cycle1];
 analogWrite(10,OCR2A);
   if(MSec101 < 5 ){
     if(PWM_Duty_Cycle1 < 49)
       PWM_Duty_Cycle1++;
   }else{
    if(PWM_Duty_Cycle1 > 0)
    PWM_Duty_Cycle1--;
   }
   ////////////////////
      if(Count1 >= 10){
  Count1 = 0;
  MSec = 1;
  MSec101++;
  //MSec101++;
  if(MSec101 == 10){
    MSec101 = 0;
```

```
      PWM_Duty_Cycle1 = 0;
      digitalWrite(F100_2, digitalRead(F100_2) ^ 1);    ///INVERT 50Hz SIGNAL
    }
  }
 /////PHASE_C PWM BY USING 0C3A PWM PIN///////
  OCR3A = SinLkUpTab[0][PWM_Duty_Cycle2];
  analogWrite(5,OCR3A);
    if(MSec10_2 < 5 ){
      if(PWM_Duty_Cycle2 < 49)
        PWM_Duty_Cycle2++;
     }else{
      if(PWM_Duty_Cycle2 > 0)
      PWM_Duty_Cycle2--;
     }
     ////////////////////
        if(Count2 >= 10){
    Count2 = 0;
    MSec = 1;
    MSec10_2++;
    //MSec101++;
    if(MSec10_2 == 10){
      MSec10_2 = 0;
      PWM_Duty_Cycle2 = 0;
      digitalWrite(F100_3, digitalRead(F100_3) ^ 1);    ///INVERT 50Hz SIGNAL
    }
  }
 ////////////////////////////////////////
}
void loop()
{
 //Main Program Here.....
}
```

Appendix B: Circuit Diagram

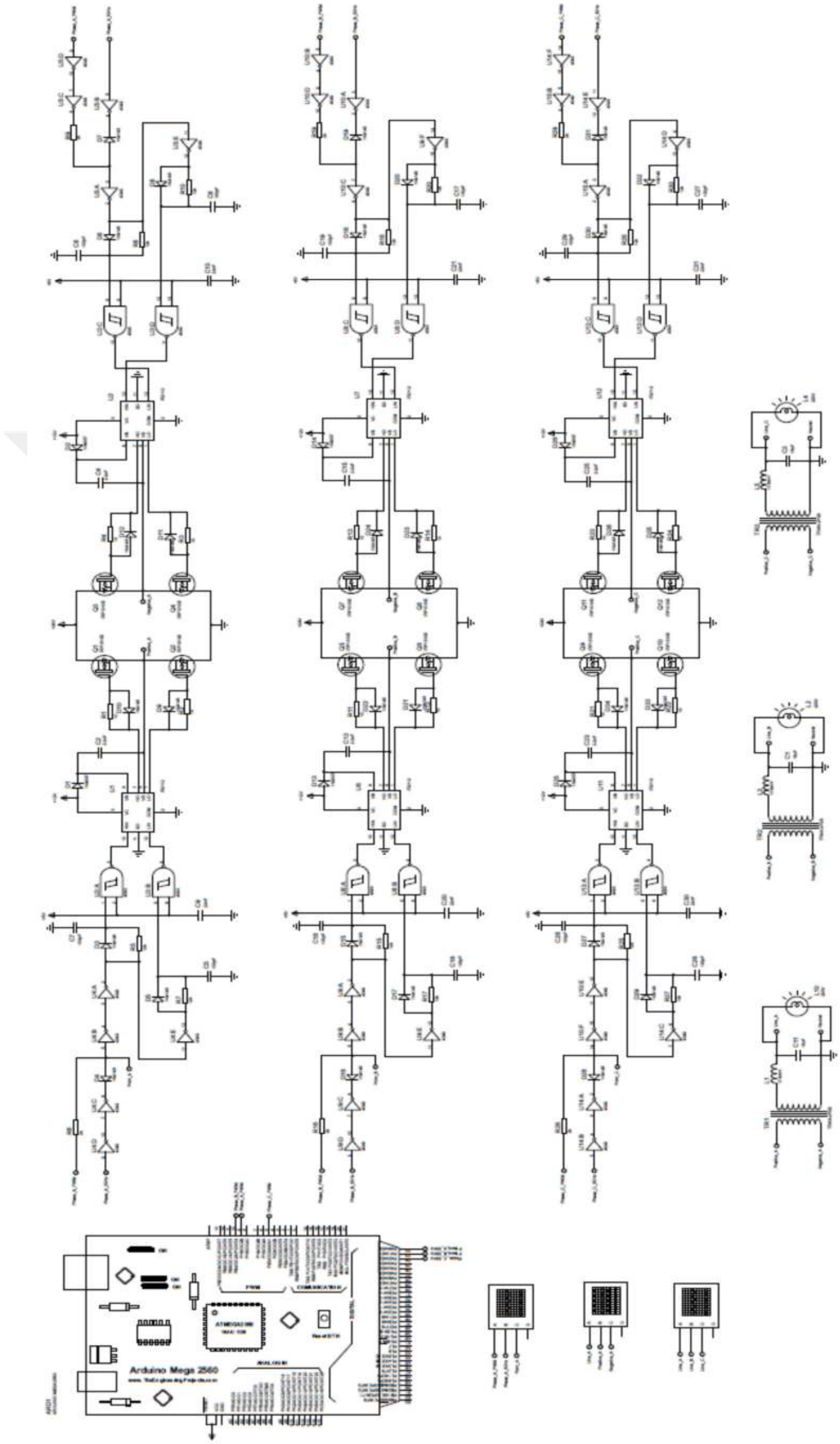

Appendix C: PCB Board Diagram

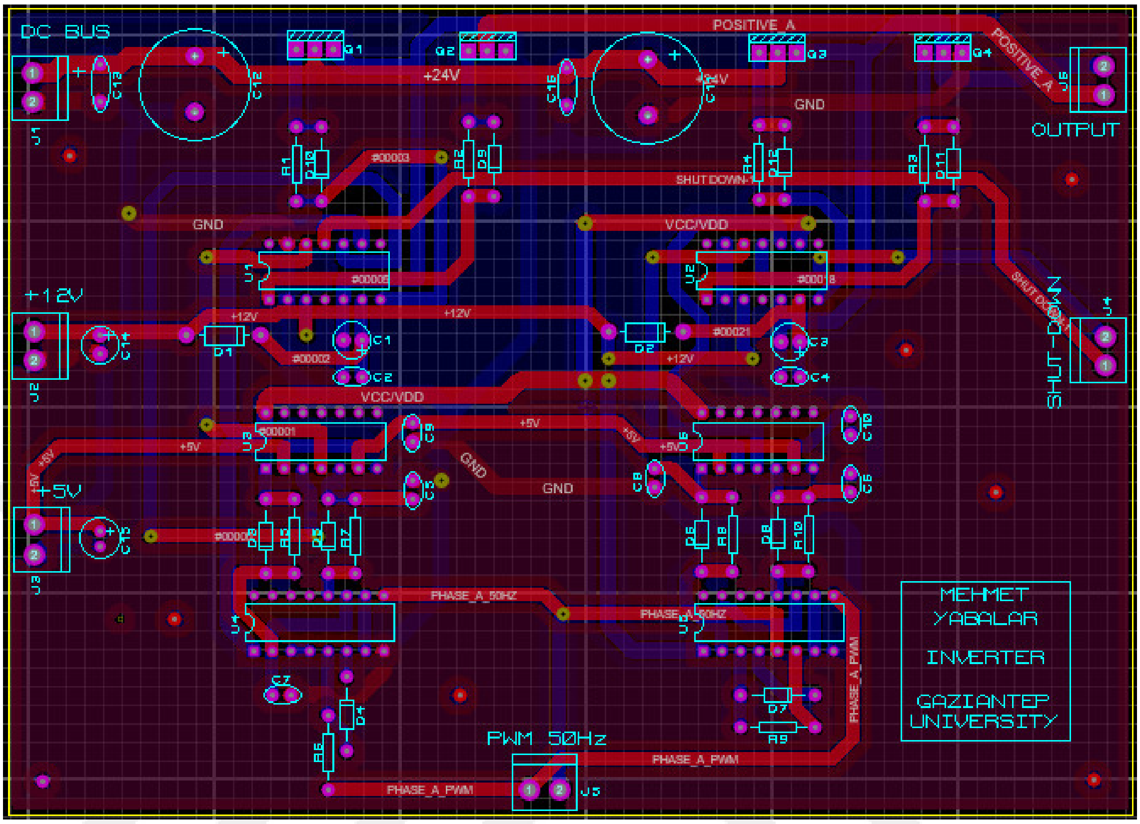

Appendix D: Parts List

#	Part Name	Piece(s)	Price	Total
1	1.5 µF 400V (Filter Capacitor)	3	0.50 $	1.50 $
2	2.2 uF Tantal Capacitor	6	0.05 $	0.30 $
3	100 pF Ceramic Capacitor	12	0.01 $	0.12 $
4	22 nF Film Capacitor	6	0.01 $	0.06 $
5	10 ohm Resistor 1/8 W	12	0.01 $	0.12 $
6	12k ohm Resistor 1/8 W	12	0.01 $	0.12 $
7	2k ohm Resistor 1/8 W	6	0.01 $	0.06 $
8	IR2112 Mosfet Driver	6	1.00 $	6.00 $
9	4093 Schmitt Trigger	6	0.10 $	0.06 $
10	4049 NOT Gate	6	0.10 $	0.06 $
11	IRF1010e Mosfet	12	0.80 $	9.60 $
12	SB1100 Schottky Diode	6	0.10 $	0.60 $
13	1N4148	30	0.01 $	0.30 $
14	Arduino Mega 2560	1	18.00 $	18.00 $
15	150 µH Filter Coil	6	1.00 $	6.00 $
16	17:220 Tranformer 200W	3	11.00 $	33 $
17	0.22 µF Snubber Capacitor	2	1.05 $	3.10 $
18	PCB Board	3	4.00 $	12.00 $
19	Cable (meter)	2	1.00	2.00 $
20	Sockets	10	0.02 $	0.2 $
			TOTAL:	**93.2 $**